

SAND90-2702  
Unlimited Release  
January 1991

Distribution  
Category UC-721

Structural Analyses and Design of a  
Concrete Liner that Limits The Disturbed Rock  
Zone Around Underground Openings in Salt

Brian Ehgartner  
Repository Isolation Systems Division  
Sandia National Laboratories  
Albuquerque, New Mexico

ABSTRACT

The mining of rooms at the Waste Isolation Pilot Plant (WIPP) creates a disturbed rock zone in the surrounding salt rock formation. The permeability of this near-field rock is higher than that of the intact rock because of fracturing, crystal misalignment, and possibly bed separation, all of which can occur upon excavation and tend to increase with time. This could result in a flow path for water and gases that may accumulate after closure of the repository and is a sealing consideration. This report discusses a new concept for a drift seal component intended to limit the formation and permeability of the disturbed rock zone; analyses of the mechanical behavior of the component are described. As envisioned, the component is a concrete liner that would be installed as soon as practical after the mining of a room, yet allow access for operational purposes. The early emplacement would slow rock deformations and exert a backpressure on the creeping salt. The result is a smaller and less permeable disturbed rock zone to seal when access to the room is no longer required.

This report examines different liner shapes, thicknesses, emplacement times, and concrete properties. Several finite-element based studies are presented that evaluate the mechanical stability of the liners, backpressures exerted by the concrete on the salt host rock, and deformation histories of the rock.

## Contents

1.0	Introduction .....	1
2.0	Constitutive Models and Properties .....	6
2.1	Constitutive Model and Properties of Salt .....	6
2.2	Constitutive Model and Properties of Concrete .....	9
2.3	Finite-Element Code .....	10
3.0	Rectangular Liner Design .....	11
3.1	Introduction .....	11
3.2	Model and Properties .....	11
3.3	Results .....	12
3.4	Conclusions .....	13
4.0	Sensitivity Study on Circular Liner Design .....	20
4.1	Introduction .....	20
4.2	Model and Properties .....	20
4.3	Results .....	23
4.3.1	Variation in Liner Thickness .....	23
4.3.2	Variation in Concrete Properties .....	25
4.3.3	Variation in Liner Emplacement Time .....	26
4.4	Conclusions .....	28
5.0	Arch-Shaped Liner Design .....	43
5.1	Introduction .....	43
5.2	Model and Properties .....	44
5.3	Results .....	45
5.4	Conclusions .....	47
6.0	Conclusions .....	55
	References .....	58
	Distribution List .....	60

## Figures

1. WIPP Facility Seal Arrangement (from Nowak, Tillerson, and Torres, 1990). . . . .	2
2. Finite Element Mesh of a 14 Ft. Wide by 13 Ft. High Room With an Optional 2.5 ft. Thick Liner. Only the upper right quadrant of the alcove is shown. . . . .	15
3. Backpressures Applied to Roof Rock After Installation of Rectangular Liner. Vertical backpressure profiles along roof rock are at 0.5, 2.5, and 5.5 years after liner emplacement. . . .	16
4. Vertical Rock Displacements Along Roof With and Without Rectangular Liner Present. Profiles represent 2.5 years after liner emplacement. . . . .	17
5. Vertical Rock Displacements at Center of Roof. Displacement histories are shown for an unlined room and with the rectangular liner installed 1.5 years after excavation. . . . .	18
6. Maximum Compressive, Shear, and Tensile Stresses in Rectangular Liner Since Time of Emplacement. Maximum compressive and shear stresses are localized at corners, whereas tensile stress is at <b>midspan</b> . . . . .	19
7. Backpressure Exerted on Rock at 1 Month, 1 Year, and 10 Years After Emplacement of Circular Liner. Liners of various thickness were emplaced 1 month after excavation of the room. . .	30
8. Backpressure Exerted on Rock For 1, 2.5, and 4 Ft. Thick Circular Liners. Liners were emplaced 1 month after excavation of the room. . . . .	31
9. Radial Rock Displacements at 1 Month, 1 Year, and 10 Years After Emplacement of Circular Liner. Liners of various thickness were emplaced 1 month after excavation of the room. . .	32
10. Radial Rock Displacement Histories for 1, 2.5, and 4 Ft. Thick Circular Liners. Also shown is 16 ft. diameter room containing no Liners. Liners were emplaced 1 month after excavation of the room. . . . .	33
11. Maximum Hoop Stresses in Circular Liner at 1 Month, 1 Year, and 10 Years After Emplacement of Liner. Liners of various thickness were emplaced 1 month after excavation of the room. . .	34
12. Maximum Hoop Stresses in Circular Liner for 1, 2.5, and 4 Ft. Thick Liners. Liners were emplaced 1 month after excavation of the room. . . . .	35

13. Backpressure Exerted on Rock at 1 Month, 1 Year, and 10 Years After Emplacement of a 2.5 Ft. Thick Circular Liner. Liners of various concrete moduli (as related to compressive strength) were emplaced 1 month after excavation of the room. . . . .	36
14. Radial Rock Displacements at 1 Month, 1 Year, and 10 Years After Emplacement of a 2.5 Ft. Thick Circular Liner. Liners of various concrete moduli (as related to compressive strength) were emplaced 1 month after excavation of the room. . . . .	37
15. Maximum Hoop Stresses in Liner 1 Month, 1 Year, and 10 Years After Emplacement of a 2.5 Ft. Thick Circular Liner. Liners of various concrete moduli (as related to compressive strength) were emplaced 1 month after excavation of the room. . . . .	38
16. Backpressure Exerted on Rock due to a 2.5 Ft. Thick Circular Liner Emplaced Prior to Room Excavation, and at 1 Month, 7 Months, 2 Years-1 Month, and 10 Years-1 Month Following Excavation. For post mining liner emplacements, room was enlarged 1 month prior to liner emplacement times. . . . .	39
17. Maximum Hoop Stresses in a 2.5 Ft. Thick Circular Liner Emplaced Prior to Room Excavation, and at 1 Month, 7 Months, 2 Years-1 Month, and 10 Years-1 Month Following Excavation. For post mining liner emplacements, room was enlarged 1 month prior to liner emplacement times. . . . .	40
18. Radial Rock Displacement Histories for a 2.5 ft. Thick Circular Liner Emplaced Prior to Room Excavation, and at 1 Month, 7 Months, 2 Years-1 Month, and 10 Years-1 Month Following Excavation. Also shown is the displacement history of a 16 ft. diameter room containing no liner. For post mining liner emplacements, room was enlarged 1 month prior to liner emplacement times. . . . .	41
19. Radial Rock Displacement Histories for 1) a 16 Ft. Diameter Circular Room, 2) the Room Enlarged 2.5 Ft. Circumferentially at 2 Years, and 3) the Enlarged Room with a 2.5 Ft. Thick Liner Emplaced 1 Month Following Enlargement. . . . .	42
20. Cross-Section of Arch-Shaped Liner Design Showing Liner and Location of Proposed Grout Holes (from Ahrens, 1990). Minimum thickness of concrete is 2.5 ft. . . . .	48
21. Finite Element Mesh Used to Model Arch-Shaped Liner. Perimeter elements (3 deep) surrounding the room modeled the liner which was emplaced 1 month after the simulated excavation of the room in salt. . . . .	49
22. Backpressure Applied to Rock at Roof, Wall, and Floor of Arch-Shaped Liner. Liner was installed 1 month after mining of room.	50

23. Rock Displacement Histories at Roof, Wall, and Floor of <b>Arch-Shaped Liner</b> . Displacement histories are also shown if no liner were emplaced in the room. Displacements are normal to boundary of room. ....	51
24. Maximum Compressive Stresses in Roof, Wall, and Floor of <b>Arch-Shaped Liner</b> . Unconfined compressive strength of concrete is also shown. ....	52
25. Maximum Compressive Stresses in 2.5 and 4.1 Ft. Thick <b>Arch-Shaped Liner Floors</b> . Unconfined compressive strength of concrete is also shown. ....	53
26. Backpressure Applied to Rock in 2.5 and 4.1 Ft. Thick <b>Arch-Shaped Liner Floors</b> . Liners were installed 1 month after mining of rooms. ....	54

## Tables

1. Mechanical Properties of Salt .....	8
2. Cases Examined in Sensitivity Study .....	22

## 1.0 INTRODUCTION

The Waste Isolation Pilot Plant (WIPP) is a facility located near Carlsbad, New Mexico, that is designed for the disposal of **defense-**generated transuranic wastes. The waste will be emplaced in underground rooms mined in salt, which has the advantage of low permeability and creep that, with time, will completely encapsulate the waste.

Before encapsulation, however, the underground openings and a localized area surrounding the openings known as the disturbed rock zone (DRZ) are potential flow paths for brine and gases. Overlying and underlying water-bearing formations and interstitial brine are potential sources of water and gases could be generated by the corrosion and biological degradation of the waste or its containers. Multi-component seals are planned to adequately control flow along these paths.

The location of proposed seals (Figure 1), and their design, function, and composition are discussed by Nowak, Tillerson, and Torres (1990). The primary long-term seal component is crushed salt. In the long term, salt creep is relied upon to consolidate crushed salt in the shafts and rooms to permeabilities essentially equivalent to those of the host rock. The short-term sealing strategy involves emplacing concrete bulkheads and plugs of bentonite to protect the consolidating long-term crushed salt in the shafts. The bentonite is expected to swell and inhibit flow if brine is introduced to the seal system. The concrete end caps confine the bentonite and are reactionary members for the swelling forces. Massive concrete bulkheads are planned for the drifts. For both the shafts and drifts, the concrete bulkheads should limit the DRZ because backpressure on the salt host rock will increase with time.

The DRZ results from the initial excavation of the underground openings and expands with time due to creep. The stress/strain redistribution due to mining of the rooms can cause fracture of the salt host rock, misalignment of the salt crystals, and bed separations, all of which may increase the permeability of the rock, thus creating potential flow

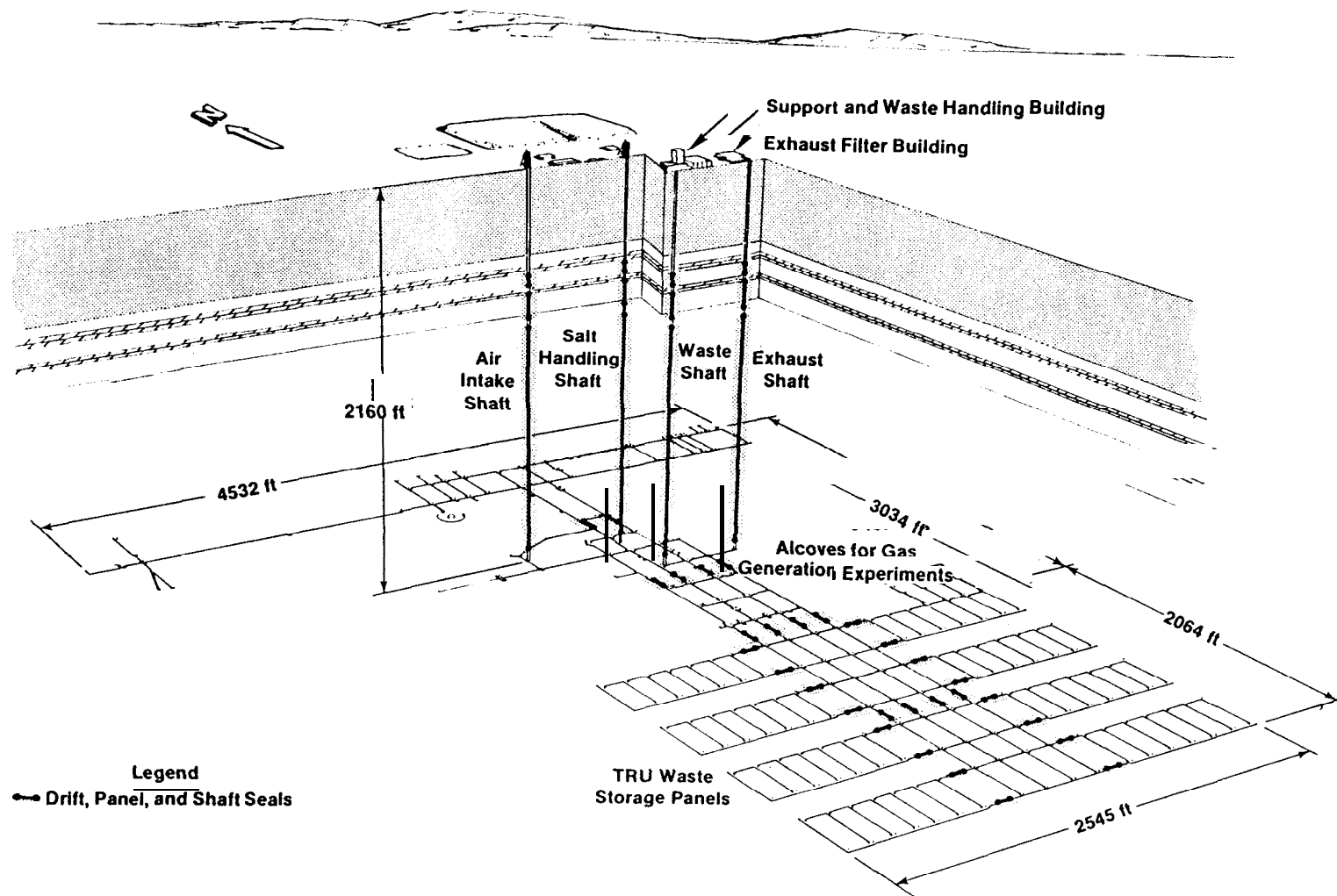


Figure 1. WIPP Facility Seal Arrangement (from Nowak, Tillerson, and Torres, 1990).

paths. As the rock creeps into the rooms, the size and permeability may increase as apertures formed by the above processes continue to open. Several approaches have been used to characterize the DRZ surrounding the excavations at the WIPP (Borns and Stormont, 1988). In general, the DRZ was found to vary in depth from 1 to 5 m depending on the size and age of the opening.

The current sealing strategy recommends the installation of panel seals as soon as possible after the waste is emplaced and the backfilling of the rooms with a crushed salt mixture. A considerable time may pass from excavation to seal emplacement thereby allowing the DRZ to develop. Room deformation rates are greatest immediately after mining of the room and the size and/or permeability of the DRZ is expected to increase with rock deformation. Therefore, a seal component is proposed to stop or inhibit this process as early as possible.

As envisioned, at the long-term seal locations, a liner would be emplaced about the perimeter of the opening. The liner would be emplaced as soon as possible after the mining of the entrance drift, and it would allow access to the waste room. When access through the liner is no longer needed, massive long-term seals would be installed. This may require removal of the liner, but portions of the liner could become part of the massive long-term seal. If the liner were removed, the backpressure exerted on the rock would be relieved and rock deformations would occur. Although this report focuses on liners installed in drifts at the repository horizon, liners could also be used in shafts to limit the development of the DRZ in salt.

This report uses the finite-element method to evaluate several liner shapes and other design parameters. The evaluation was based on the ability of the liner to apply significant backpressure to the rock, inhibit or stop rock deformations, and remain mechanically stable. For this report, the following three design criteria were considered (as the design progresses, more criteria may be added):

1. The liner should apply significant backpressure to the salt host rock. Backpressure is a reaction of the liner due to creep of the salt host rock and therefore is a function of time. The amount and duration of backpressure required to heal or partially heal a characteristic aperture in the DRZ is not explicitly known at this time.
2. The liner should limit host rock deformation. Stress relief associated with the mining and subsequent creep of the host rock tends to open apertures in the DRZ. With time, a larger DRZ and/or greater aperture sizes in the DRZ are expected. This process is assumed to be limited if the rock deformations are limited.
3. The liner must be structurally stable. In these analyses, the concrete liner is assumed to be elastic, and it undergoes compressive loading due to the creep of the host rock. The stability criteria are based on comparing the liner stresses to the strength of the concrete. In these initial design calculations, a liner was defined as structurally stable when the stresses were less than the strength of concrete. Later, as the design progresses, a suitable safety factor should be defined and incorporated into the stability criteria.

The most immediate potential application of the liner in the WIPP is probably the closing of long alcoves in which the gas-generating potential of waste is to be assessed (Molecke, 1990). Four alcoves, each approximately 170 ft. long and 14 ft. wide by 13 ft. high (rectangular cross sections), exist for experimental purposes. These extend off the northern portion of Panel 1 and are opposite the rooms of the panel (Figure 1). Because the alcoves have been open for over a year and a half, and measurable bed separations have occurred in the DRZ surrounding the alcoves, consideration will have to be given to grouting the DRZ after installing a liner or to mining new rooms for the **gas-generation** experiment.

The first design (Chapter 3) considers emplacing 2.5 ft. thick rectangular liner in the alcoves 1.5 years after the alcoves are mined. This option was considered the simplest liner to design and construct. To better understand how the major design parameters affect liner performance, a sensitivity study was performed (Chapter 4). The sensitivity of a ring-shaped liner installed in a circular room to various liner thicknesses, and differing concrete properties and installation times was studied. Based on the results of the above studies and taking into consideration mining, concrete placement, and grouting aspects (Ahrens, 1990), an arched room and liner design was evaluated (Chapter 5).

The constitutive models and properties used in the analyses are defined in Chapter 2. The report concludes (Chapter 6) by passing on valuable concepts and information gained from the studies. Each of the analysis chapters (3 through 5) are structured similarly: introduction, discussion of the finite-element model and material properties, analysis results, and conclusions.

## 2.0 CONSTITUTIVE MODEL AND PROPERTIES

This chapter discusses the constitutive models and properties used to represent the mechanical behavior of the salt host rock and concrete liners. The finite-element computer code used for the analyses is also discussed.

### 2.1 Constitutive Model and Properties of Salt

The salt behavior was represented by the Munson-Dawson creep model and properties, which is a Multimechanism Steady State Workhardening/Recovery Model as originally developed by Munson and Dawson (1979) and later modified to provide a more descriptive transient strain function (Munson, Fossum, and Senseny, 1989a,b). The model incorporates the Tresca flow potential and is based on micromechanistic concepts using a deformation mechanism map (Munson, 1979). The mechanism map defines regions of stress and temperature in which a unique deformation mechanism controls or dominates steady-state creep. The model identifies three steady-state mechanisms: Mechanism 1 dominates at high temperatures and low stresses; Mechanism 2 dominates at low temperatures and stresses; and Mechanism 3 dominates at high stresses at all temperatures. Mechanism 2 dominates the analyses performed in this report because elevated temperatures were not modeled. The steady state strain rates for Mechanisms 1 and 2 are equal to:

$$\dot{\epsilon} = A e^{(-Q/RT)} s^n,$$

where A is a constant, Q is the activation energy, T is the absolute temperature (300 K), R is the universal gas constant (1.987 cal/mol-K), s is the generalized stress, and n is the stress exponent. The form is similar to that of the 1984 reference creep law (Krieg, 1984).

Transient creep is included in the model through a function composed of a workhardening branch, an equilibrium branch, and a recovery branch.

The details of this component and the steady-state component of creep are discussed by Munson, Fossum, and Senseny (1989a).

The salt properties in the analyses were based on a reevaluation study by Munson, Fossum, and Senseny (1989a,b). The value used for the transient strain limit (K) differs slightly from the published data of the reevaluation study as a result of subsequent refinement of test data (Munson, 1989). The values reflect combined data from the original ERDA-9 data base and additional data from creep tests made on core from the facility horizon (Senseny, 1990). The reevaluated parameter set is listed in Table 1 for argillaceous halite. The stratigraphy (Munson, Fossum, and Senseny, 1989a,b) was modeled as argillaceous halite because the salt is predominantly argillaceous, **surrounding** the proposed liner locations. The most noticeable exception is Marker Bed 139, a 2.5 ft. thick anhydrite layer approximately 4.5 ft. under the floor of the rooms in the waste disposal area.

The constitutive model is intended to represent the intact behavior of salt, and the properties are based on laboratory tests. Therefore, the DRZ is not modeled in the analyses performed in this report. Because the effect of the DRZ on liner behavior is ignored in this study, the actual time required to reach the predicted rock and liner pressures may be slightly more than predicted. The partings and apertures in the DRZ will tend to soften the overall modulus of the rock. However, as the DRZ heals and the partings and cracks begin to close, the DRZ should behave more like the intact salt. Conversely, it can be argued that the DRZ will tend to creep faster than intact rock and load the liner more quickly. However, this does not appear to be the case, as measured room closures agree rather well with those predicted using the above model and properties.

The Munson-Dawson creep model is presently being evaluated with underground data in a preliminary validation exercise. Preliminary results show good agreement in predicted room closure with that measured in Rooms D, B, G, and the South Drift of the WIPP (Munson, Fossum, and Senseny, 1989a,b; Munson and DeVries, 1990).

Table 1  
Mechanical Properties of Salt\*

---

Elastic Properties			
Poisson's ratio		0.25	
Modulus of elasticity (E)		31.0 GPa	
Creep Properties			
Steady-state Mechanism 1		Steady-state Mechanism 2	
<b>A<sub>1</sub></b>	1.407 E23 /s	<b>A<sub>2</sub></b>	1.314 E13 /s
<b>Q<sub>1</sub></b>	25000 cal/mol	<b>Q<sub>2</sub></b>	10000 cal/mol
<b>n<sub>1</sub></b>	5.5	<b>n<sub>2</sub></b>	5.0
Steady-state Mechanism 3		Transient creep	
<b>B<sub>1</sub></b>	8.998 E6 /s	<b>m</b>	3.0
<b>B<sub>2</sub></b>	4.289 E-2 /s	<b>K</b>	1.783 E6
<b>sig<sub>0</sub></b>	20.57 MPa	<b>c</b>	0.009198 /T
<b>q</b>	5.335 E3	<b>a</b>	-14.96
		<b>b</b>	-7.738
		<b>d</b>	0.58

\* For a complete definition of the above parameters see Munson, Fossum, and Senseny, 1990a.

---

## 2.2 Constitutive Model and Properties of Concrete

Concrete was modeled as an elastic material with a modulus equivalent to the salt host rock (31 **GPa**) and a Poisson's ratio of 0.2. The density of concrete was assumed to be 145 **lb/ft<sup>3</sup>**. The unconfined compressive strength of concrete was estimated as 43 **MPa** or 6200 psi based on the modulus/strength relationship recommended in **ACI 318-7** (**Thorton** and Lew, 1983). This same relationship was used in the sensitivity study, Chapter 4, to vary the modulus (21.5 to 37.3 **GPa**) and hence strength of the concrete (3000 to 9000 psi). The modulus as related to the unconfined compressive strength is

$$E = 57,000 (\text{strength})^{0.5},$$

where strength is the compressive strength in psi and E is the secant modulus of elasticity in psi. The shear strength of concrete was assumed to be one-sixth of the compressive strength and the tensile strength of concrete was assumed to be equal to one-tenth of the compressive strength.

These strength relationships, which are typical for plain concrete, are considered adequate for initial design purposes. The addition of reinforcement, such as rebar, could enhance the shear and particularly the tensile strength of the concrete. Once the concrete formulation is decided, the properties should be defined through testing.

The salt and concrete were modeled as perfectly bonded materials with no frictional interface or sliding permitted. The properties of concrete were assumed to be constant with time, although it is recognized that in practice it takes approximately a month for the concrete to harden and both strength and modulus increase with age.

### 2.3 Finite-Element Code

The previously described constitutive models and properties were used in the SPECTROM-32 code (RE/SPEC, 1989) to perform the calculations. The code is a two-dimensional finite-element thermomechanical stress analysis program written to solve nonlinear, time-dependent rock mechanics problems.

The following calculations simulated up to 10 years following emplacement of the liner.

## 3.0 RECTANGULAR LINER DESIGN

### 3.1 Introduction

This chapter documents two finite-element analyses performed to evaluate the mechanical response of a 2.5 ft. thick concrete liner emplaced in a 14 ft. wide by 13 ft. high room. The utility of the liner in limiting rock displacements and generating backpressure on the disturbed rock zone (DRZ) is scoped. The first analysis models the rectangular room without the liner, and the second analysis models the room with the concrete liner added 1.5 years after excavation of the room. This particular design was chosen for analysis because it is the simplest. No additional mining is required and the concrete pour is uniform in thickness. The geometry reflects that of the long test alcoves north of Panel 1 (Figure 1) to be used for the gas-generation experiments.

### 3.2 Model and Properties

The finite-element mesh (67 ft. wide by 63 ft. high) used for both calculations is shown in Figure 2. A 2-D representation of the rooms implies that they are long with respect to their cross-sectional dimensions. Similarly, the concrete liner is assumed to be relatively long. The mesh contains 216 elements and 247 nodal points.

**Rollered** boundary conditions were applied at the sides and bottom of the mesh to model symmetry. As such, only a quarter of the room is represented by the mesh, and the predicted behavior of the roof and floor will be identical in these scoping calculations. The boundary conditions represent an infinite series of rooms separated by 119 ft. wide pillars. The geometry simulates that of the test alcoves north of Panel 1 (Figure 1). However, only 4 alcoves, each approximately 170 ft. **long**, exist for experimental purposes. An initial pressure of 14.31 MPa was applied to the top of the mesh and a gradient resulted in a

lithostatic pressure of 14.76 MPa at the bottom of the mesh.

The darkened area in Figure 2 shows the elements that simulated the concrete emplacement 1.5 years after excavation. The liner was emplaced about the perimeter of the room, so the inside working dimensions of the room would be reduced.

The Munson-Dawson creep model and salt properties described in Chapter 2 were used to model the salt. The concrete was modeled as an elastic material using the properties defined in Chapter 2.

### 3.3 Results

Figure 3 shows the calculated backpressures exerted by the concrete room on the roof rock at 0.5, 2.5, and 5.5 years after emplacement. The vertical stresses increase with time at all locations along the roof. The backpressures are lowest at mid-span and increase to maximum at approximately 1.5 m from the center of the room. This distance corresponds to the area over the wall concrete that in part supports the roof. The maximum backpressure approaches but does not quite reach lithostatic pressure (14.76 MPa) at 5.5 years after emplacement. The backpressures are considered significant in that partial healing of the DRZ could occur with time under such loads.

Figure 4 shows the vertical roof displacements along the top of the room for both analyses at 2.5 years after liner emplacement. As expected, the largest sag occurs in the center of the room whether the concrete liner is present or not. However, the displacements are much less for the room with the 2.5 ft. thick concrete liner added. This effect is better illustrated in Figure 5.

Figure 5 shows the vertical displacement history at the center of the room for both the lined and unlined room. In both cases, the displacement histories are equivalent up to 1.5 years after excavation.

At that time, the liner is emplaced in the one analysis. The vertical displacements remain essentially constant after installation of the concrete liner, whereas they continue to increase in the unlined room. Because roof deformation is (for practical purposes) stopped due to the installation of the liner, the growth of the DRZ surrounding the room should be limited, if not stopped. This figure also shows the large amounts of deformation that occur relatively quickly after excavation. Because DRZ growth may be proportional to deformation, it may be desirable that the concrete liner be installed as soon as possible after mining.

Figure 6 shows the maximum compressive, shear, and tensile stresses at any location in the concrete liner for 8 years following its emplacement. The maximum compressive and shear stresses occur at the inside corners of the concrete liner. These stresses quickly exceed the strength of concrete (43 MPa), but the high stresses are local to the corners. At **midspan**, the tensile stress (due to a beam bending effect) does not exceed 1.2 MPa over the 8 years shown. The maximum tensile stress is well below the assumed tensile strength (4.3 MPa).

The above results concentrate on the roof behavior, although the roof and floor are predicted to behave identically because of model symmetry. Results for the wall areas do not differ largely from those reported for the roof/floor areas because of the approximately square shape of the the room. Deformations tend to be slightly less in the wall areas.

### 3.4 Conclusions

The results show that roof deformation is essentially stopped and that significant backpressures are exerted on the rock due to the addition of the concrete liner. By stopping roof deformation, the growth of the DRZ surrounding the room should be limited. The backpressures that are generated because of the concrete may act to heal portions of the DRZ

with time. The calculations also illustrate the desirability of installing the concrete liner as soon as possible after excavation.

This particular design was chosen for analysis because it is the simplest. However, localized failure of concrete in the corners of the liner was predicted. A potentially advantageous design would round both the inside and outside corner to help alleviate stress concentrations there, and thicken the **midspans** to produce a more uniform backpressure. Because of the initial hydrostatic stress state, a circular or **ring-shaped** design would be better from a stress point of view. This shape is considered in Chapter 4, where a sensitivity study is performed on the major design variables as well.

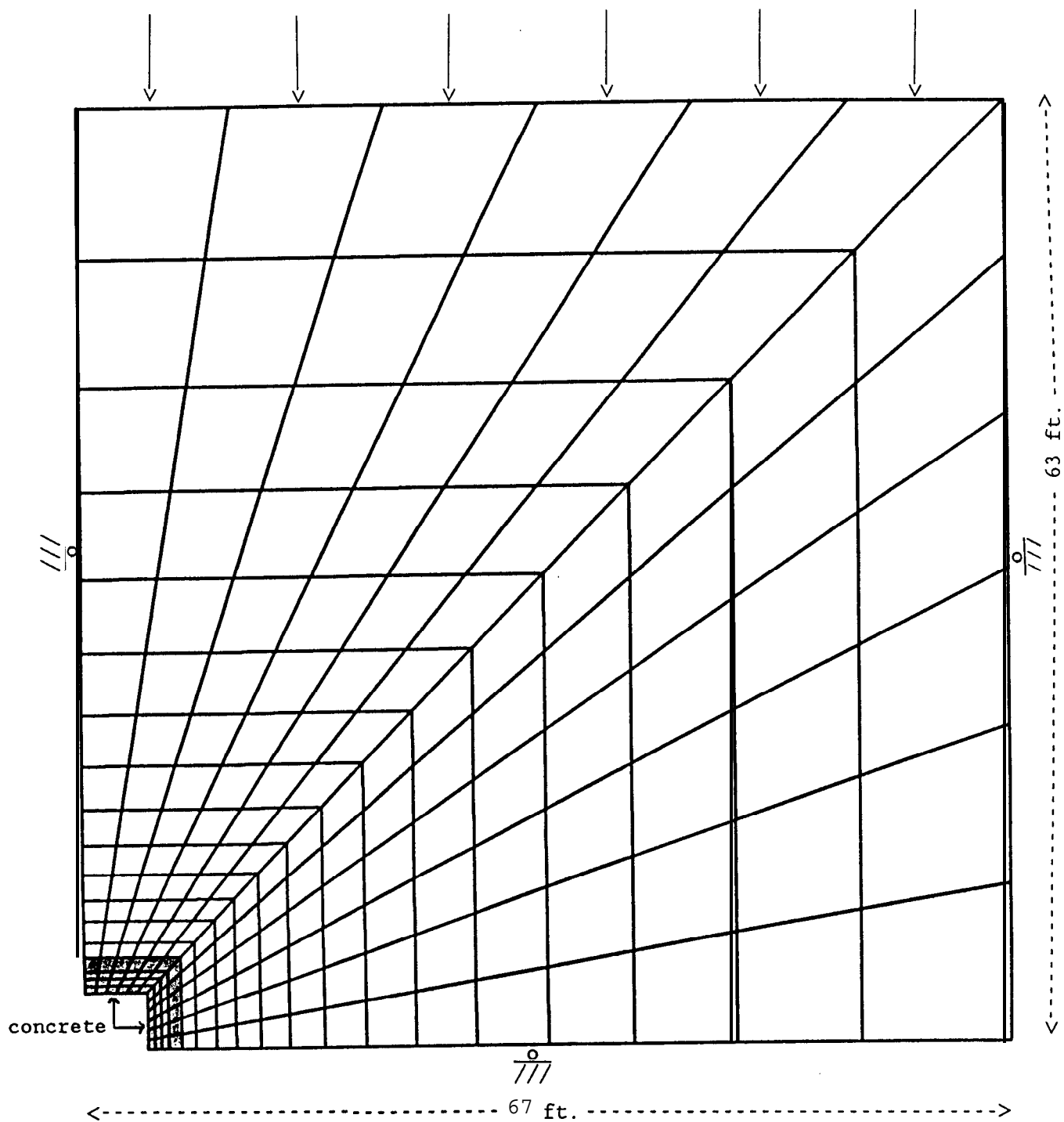


Figure 2. Finite Element Mesh of a 14 Ft. Wide by 13 Ft. High Room With an Optional 2.5 ft. Thick Liner. Only the upper right quadrant of the alcove is shown.

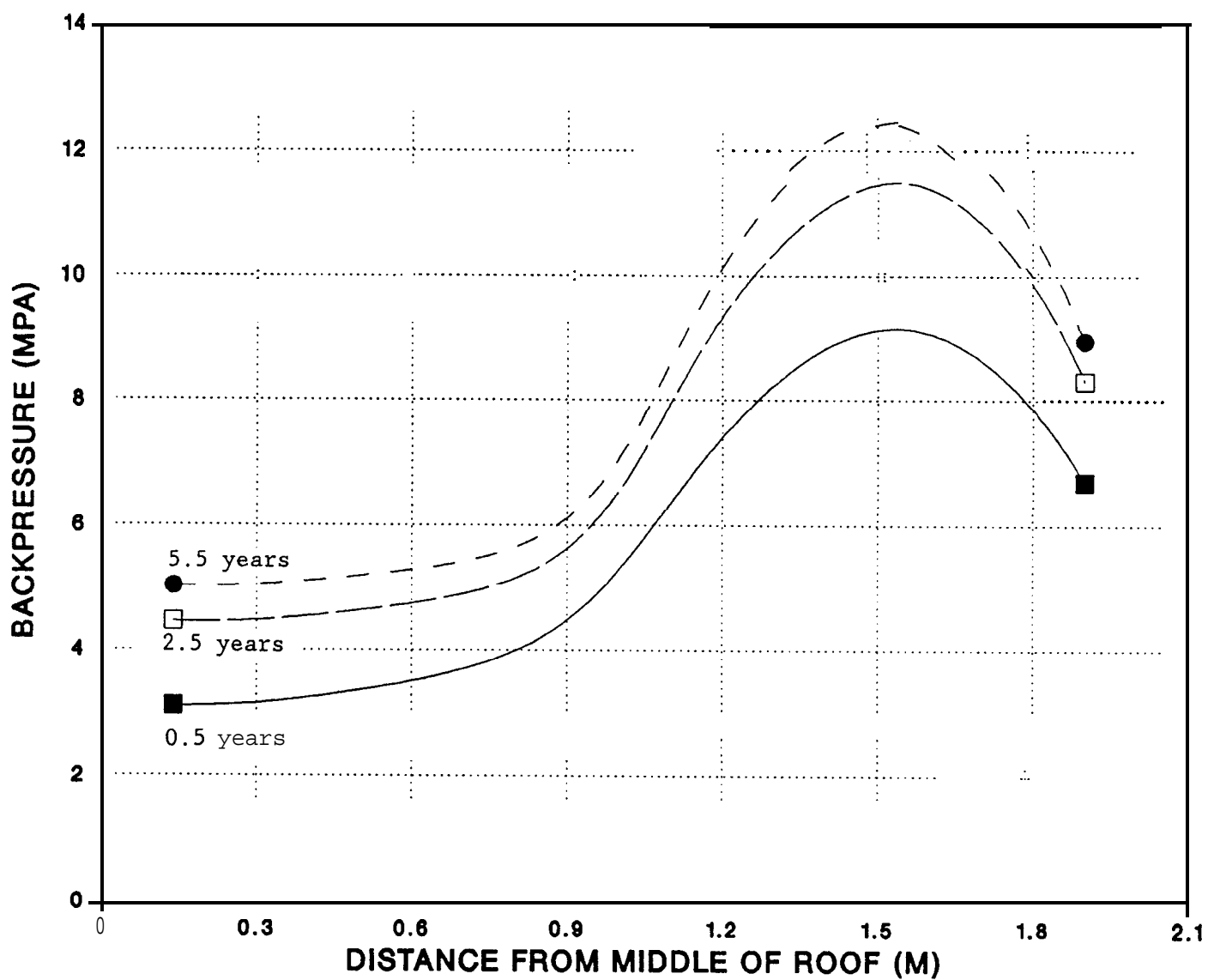


Figure 3. Backpressures Applied to Roof Rock After Installation of Rectangular Liner. Vertical backpressure profiles along roof rock are at 0.5, 2.5, and 5.5 years after liner emplacement.

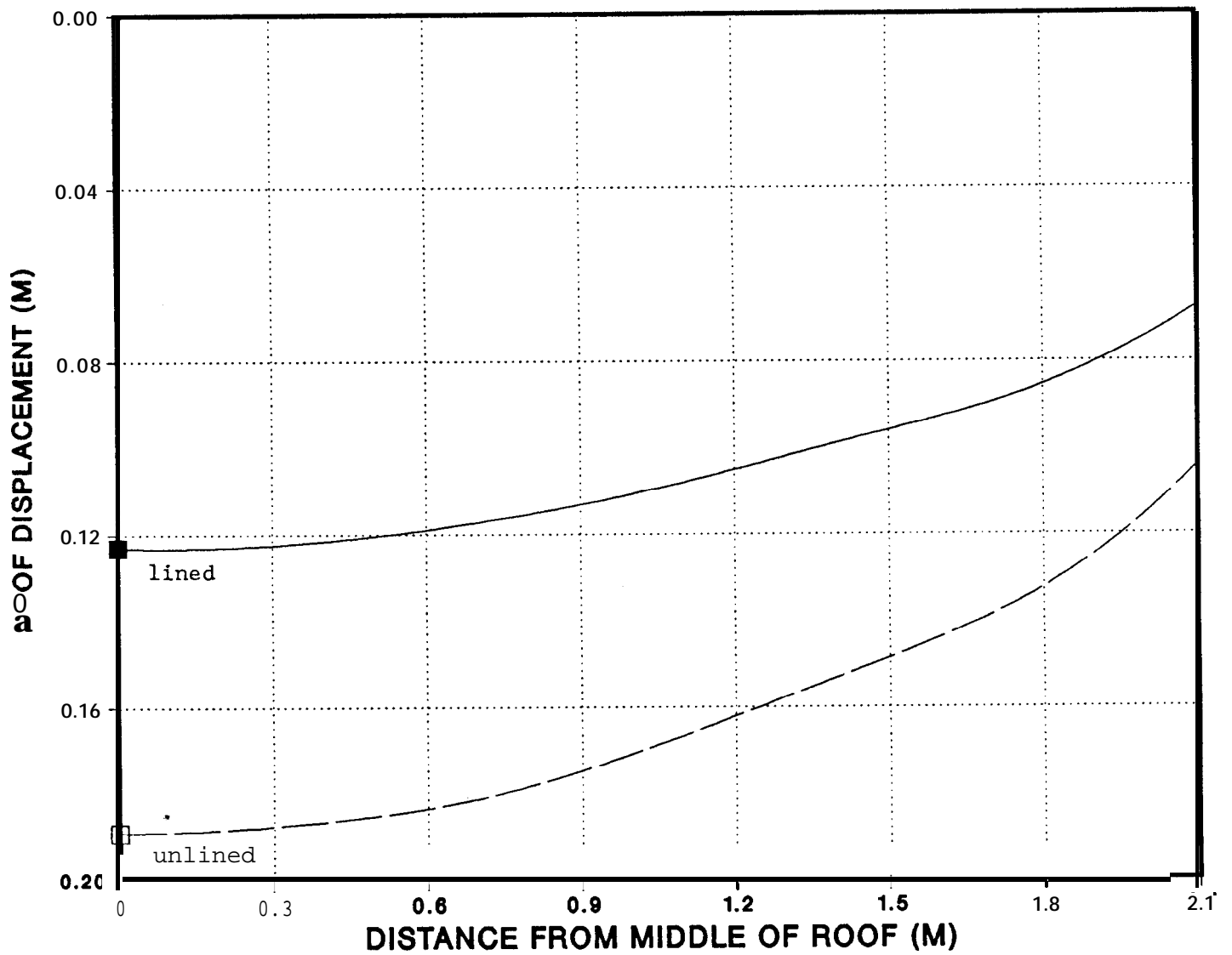


Figure 4. Vertical Rock Displacements Along Roof With and Without Rectangular Liner Present. Profiles represent 2.5 years after liner emplacement.

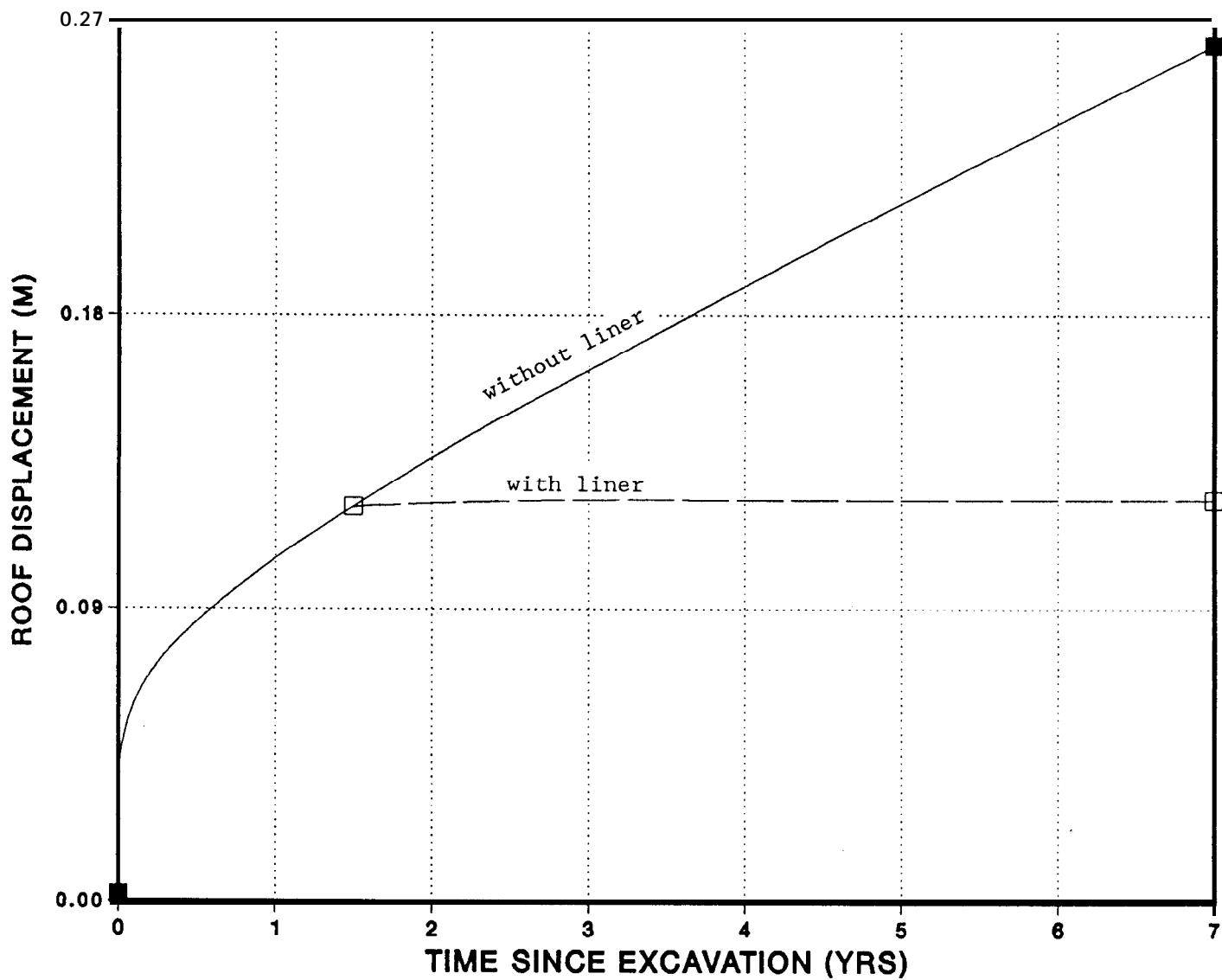


Figure 5. Vertical Rock Displacements at Center of Roof. Displacement histories are shown for an unlined room and with the rectangular liner installed 1.5 years after excavation.

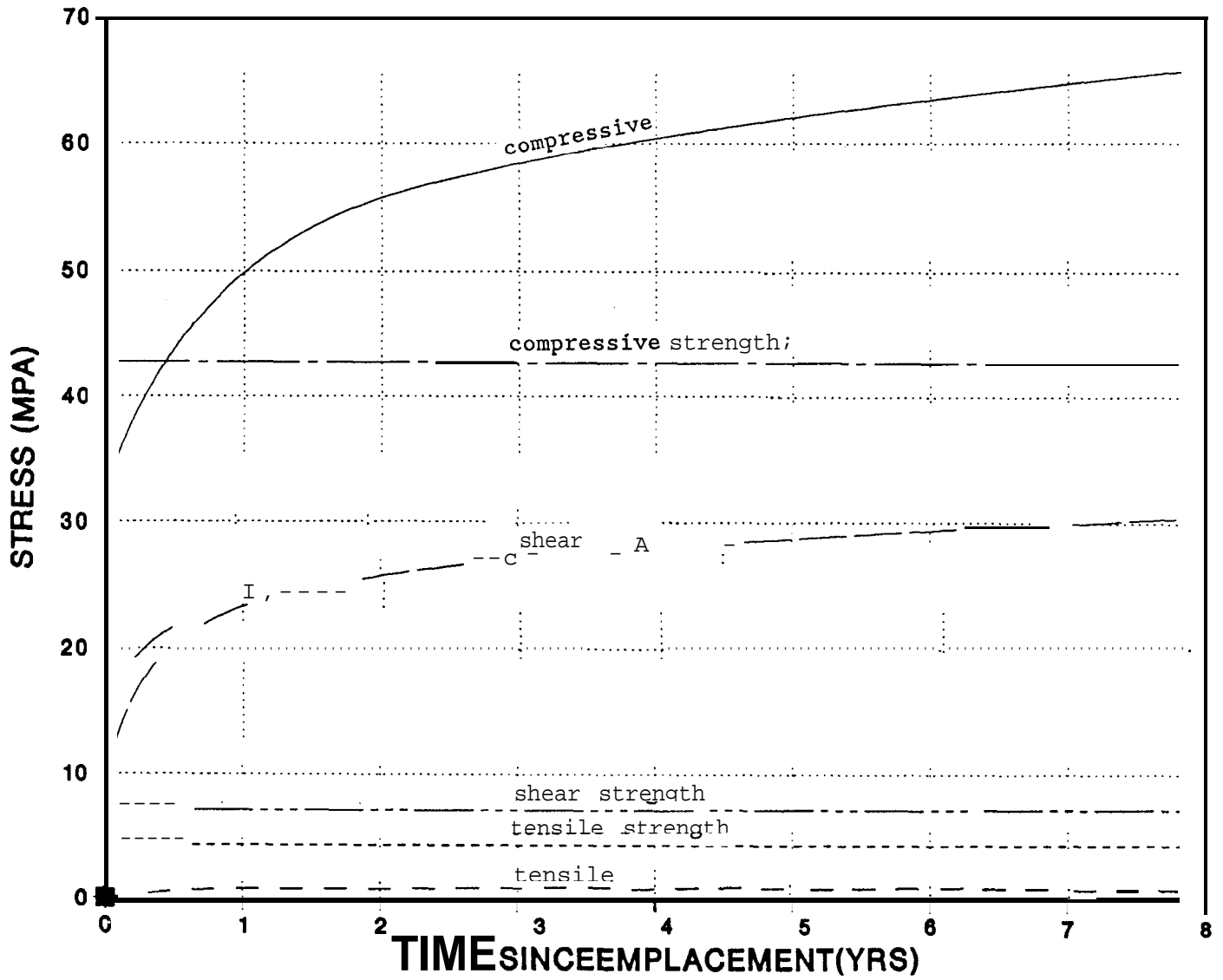


Figure 6. Maximum Compressive, Shear, and Tensile Stresses in Rectangular Liner Since Time of Emplacement. Maximum compressive and shear stresses are localized at corners, whereas tensile stress is at midspan.

## 4.0 SENSITIVITY STUDY ON CIRCULAR LINER DESIGN

### 4.1 Introduction

The sensitivity of the mechanical response of an annular concrete liner emplaced in a circular underground room or alcove to various liner thickness, concrete properties, and installation times is evaluated. The analyses examine the liner stresses, the backpressures they exert on the rock, and the rock displacement histories for the various cases over 10 simulation years. The results are useful in designing room or alcove liners in which the emphasis is on limiting the extent of the disturbed rock zone (DRZ).

### 4.2 Model and Properties

A circular 16 ft. diameter room 2135 ft. below the surface was simulated in the analyses. The opening was then enlarged to accommodate an annular concrete liner emplaced 1 month after mining. A 16 ft. diameter opening with a flattened floor has approximately the same **cross-sectional** area as the 13 ft. high by 14 ft. wide alcoves needed for the gas generation experiments (Molecke, 1990). This study models a single isolated room, whereas 6 alcoves are needed for the gas-generation experiments. Although a 16 ft. opening was selected for evaluation, the results of this study are applicable to other diameter openings, since the resulting stress/strain fields are solely dependent upon the ratio of liner thickness to opening size.

The sensitivity of liner thickness, its properties, and emplacement times were evaluated. Liner thickness varied from 6 in. to 4 ft. The concrete strength and its corresponding elastic modulus was varied to represent unconfined compressive strengths from 3000 to 9000 psi. The corresponding elastic modulus was calculated from the following relationship (ACI 318-7, **Thorton** and Lew, 1983; also Chapter 2):

$$E = 57,000 (\text{strength})^{0.5},$$

where strength is the compressive strength in psi and E is the secant modulus of elasticity in psi.

The liners were simulated as being installed approximately 1 month (31 days) after enlarging the 16 ft. opening to accommodate the liners. The time at which the enlargement occurred was varied from 0 to 10 years after the original mining of the room. In one case, the liner was assumed to exist prior to the original mining of the room. This case allowed the elastic response of the room to initially load the liner upon mining of the room. Although recognized as unrealistic, it can represent an upper bound to liner loading. Such conditions may be approached when a liner is installed at the face of a room and, allowed to set, and then mining of the room resumes. Table 2 lists the different cases analyzed.

Because of the circular geometry, the problem was idealized as 1-D axisymmetric, which results in a room and liner that are infinitely long. Therefore, room-end effects are ignored. The finite-element mesh consisted of 109 elements extending out a radial distance of 210 ft. The aspect ratio of the first 8 elements (to 12 ft.) was equal to 1. The aspect ratio was then progressively increased until reaching the boundary. The elements were restrained to only lateral motion, and a constant pressure of 14.76 MPa was applied to the outermost element.

The Munson-Dawson creep model and salt properties described in Chapter 2 were used to model the salt. The concrete was modeled as an elastic material, using the properties defined in Chapter 2 for the base case.

Table 2  
Cases Examined in Sensitivity Study

Study No.	Liner Thickness (ft.)	Liner Strength (psi / MPa)	Liner Modulus (GPa)	Time of Room Enlarging (yrs)
1	0 (no liner)	6220 / 42.9	31	0
	.5			
	1			
	1.5			
	2			
	2.5			
	3			
	3.5			
	4			
2	2.5	3000 / 20.6	21.5	0
		5000 / 34.5	27.8	
		6220 / 42.9	31.0 (same as salt)	
		7000 / 48.3	32.9	
		9000 / 62.0	37.3	
3	2.5	6220 / 42.9	31.0	0 *
				0
				0.5
				2
				10

\* includes loading from elastic relaxation of room due to mining.

### 4.3 Results

The variation of backpressure, rock displacement, and liner hoop stresses to changes in liner thickness, concrete properties, and liner emplacement time are examined in each of the following sections. Backpressure is the radial stress exerted on the rock due to the presence of the concrete liner. Backpressure may help heal fractures that can develop around the room after its mining. The rock displacements are located at the interface of the liner and rock. The ability of a liner to limit rock displacement may result in its retarding the magnitude and extent of the DRZ. Because of the circular geometry and load symmetry assumed in the analyses, only compressive hoop stresses are of concern to structural stability. In these analyses, liner hoop stresses are highest at the inner surface of the liner and are therefore reported below.

#### 4.3.1 Variation in Liner Thickness

Figure 7 shows the variation in liner pressure applied to the rock (e.g., backpressure) as a function of liner thickness at 1 month, 1 year, and 10 years after emplacement of the liner in the room. The liner was emplaced 1 month after the simulated mining of the room. Backpressure increases nonlinearly with liner thickness at all installation times. The increase is less dramatic at later installation times. Most of the backpressure is realized for a liner approximately 2.5 ft. thick.

Figure 8 shows the development of backpressure with time for the 1, 2.5, and 4 ft. thick liners. The backpressure develops quickly within the first year, and then levels off with time. The thicker liners tend to load the rock at a quicker rate than the thinner ones. For the 2.5 ft. thick liner, approximately 50 percent of the 10 year backpressure is developed at about 1 month after liner emplacement. The final backpressure is approximately 44 percent of lithostatic pressure (14.76 MPa).

Figure 9 shows the radial or inward displacements of the rock for the liners. In general, as the liner becomes thicker, the displacements are larger. Larger displacements are associated with the bigger excavations required to accommodate the thicker liners. In terms of absolute rock displacements, the results show that the thinner liners are better. The reverse trend would be noted if the outside dimension of the excavation, instead of the inside dimension, had remained constant over the various cases. In terms of relative displacements after the liners are installed, the changes in rock displacements are least for the thicker liners. For a 2.5 ft. thick liner, the rock displaces only 0.0023 m (0.092 in.) over 10 years after its emplacement.

Figure 10 shows the time history of rock displacement for 1, 2.5, and 4 ft. thick liners emplaced 1 month after room excavation. Also shown are the rock displacements for an unlined room (e.g., no liner or enlarging). The displacements are essentially halted by the emplacement of the liner in all cases. As mentioned above, the thicker liners required a larger excavation, so the displacements are larger in magnitude. At approximately 9 months, the benefit of the 2.5 ft. thick liner is realized because the absolute displacements for the unlined room are larger than those of the lined room.

Figure 11 shows the maximum hoop stress of the concrete liner as a function of liner thickness. The thicker liners result in less stress, regardless of time but especially later. Liners less than 1 ft.- 8 in. are predicted to fail after 10 years of emplacement as the estimated strength of the concrete is approximately 43 MPa. Up to 1 year after emplacement, a 1 ft. thick liner would just be acceptable. The high hoop stress appears to be moderated once the liner is approximately 2.5 ft. thick.

Figure 12 shows the increase in hoop stress with time for 1, 2.5, and 4 ft. thick liners. The trend is similar to backpressure, except much larger spreads in stress are noted between the various liner thickness. After 1 month, the hoop stresses for the 1 ft. thick liner are at least

twice those of the 4 ft. thick liner. At 10 years, this amounts to a predicted difference of 38 **MPa**, whereas the difference in backpressure was only 0.5 **MPa** (Figure 8) at 10 years.

#### 4.3.2 Variation in Concrete Properties

Figure 13 shows the change in backpressure due to variation in the modulus (21.5 to 37.3 **GPa**) and hence strength of the concrete at 1 month, 1 year, and 10 years after liner emplacement. Only a slight increase in backpressure is noted over the range of moduli analyzed. The difference in backpressures ranged from 0.4 **MPa** at 1 month to only 0.1 **MPa** at 10 years. Backpressure does not appear to be sensitive to changes in concrete moduli.

Figure 14 shows the absolute rock displacements as a function of moduli. The largest range in displacement, noted at 10 years, is 1.4 mm over the range of moduli. This is less than a 3 percent increase in deformation. As expected, the displacements increase with softer concrete moduli.

Figure 15 plots the maximum hoop stress in the concrete liner over the range of moduli examined. Also shown in the figure is the compressive strength of the concrete. The hoop stresses increase as the liner stiffness increases, but the increases are almost negligible one year after emplacement. The greatest sensitivity is noted at the earlier times. At 1 month, a 2.1 **MPa** or 18 percent increase can occur. Strength increases much more quickly with increases in moduli than does the hoop stress, so a high moduli concrete is desirable. The hoop stresses are less than the strength of concrete for the 2.5 ft. thick liner where the modulus is greater than 26 **GPa**. As with the trends for backpressure, these trends are nonlinear, although they appear linear on the figures.

#### 4.3.3 Variation in Liner Emplacement Time

Figure 16 shows the variation in backpressure for liners emplaced at 1 month, 7 months, 2 years and 1 month, and 10 years and 1 month after initial mining of the room. The enlarging of the room to accommodate the 2.5 ft. thick liner occurred 1 month before liner emplacement. Also shown is a case in which the liner was emplaced before mining of the room. This case was included to provide an upper bound on liner backpressure.

The full elastic relaxation of the room due to mining is imposed on the liner. Such a condition could only be approached if special liner installment techniques were used. The liner would have to be immediately emplaced at the face and allowed to harden (taking approximately 1 month) before the room was advanced. The backpressures for this case are much higher than any of the cases in which the liner was installed after mining. For emplacement after mining, a less than 1 **MPa** difference is noted in the cases. The backpressures develop more quickly in those liners installed earliest.

Figure 17 shows the maximum hoop stresses developed in the concrete liners for the various emplacement times. The estimated compressive strength of the concrete (based on a 31 **GPa** modulus) is also shown. In all cases, except when the liner was emplaced before mining, the hoop stresses are well below the compressive strength of the concrete (43 **MPa**) up to 10 years after liner emplacement. As shown in Figure 16, the emplacement of the liner prior to mining resulted in significantly higher stresses that quickly exceed the compressive strength of the liner. The hoop stresses of the other cases vary by approximately 3 **MPa** at 10 years after liner emplacement. The hoop stresses at later emplacement times are higher than some of those at earlier times, which appears to conflict with the radial back pressures that decrease with later emplacement times (Figure 16). This is a result of model boundary effects. A similar effect would be noted underground as the excavation of nearby rooms decreases the radial component of stress and increases

the tangential stress.

Figure 18 shows the rock deformation for the above cases. In addition, the deformations of an unlined room are shown to provide perspective on the utility of emplacing a liner. The initial location of the rock does not change for the unlined room: it is 8 ft. from the centerline of the circular room. However due to enlarging of the room to accommodate the 2.5 ft. thick liner, the dimension of the room changes. It increases from 8 ft. to 10.5 ft. from the room centerline. As such, the displacement history appears to be discontinuous in the figure. The displacement histories for the liner/rock interface start at the time of enlarging. Hence there is an initial jump in displacements due to the enlarging of the opening-- an initially elastic response followed by transient creep. As illustrated, the displacements become relatively constant in a short time, which corresponds to the emplacement of the liner, 1 month after enlarging. It is interesting to note that for some of the early installation times, the enlarging and emplacement of the liner results in initially greater displacements than if no liner were installed in the room. This condition is short lived though. For all emplacement times, the benefit of emplacing a liner is realized. The earlier a liner is installed, the less total rock displacement occurs. In all cases, displacements are significantly reduced due to liner emplacement.

Figure 19 better illustrates the effectiveness of a liner in reducing rock deformations and the impact of enlarging the room to install the liner. The displacement histories as shown for a 16 ft. diameter room, that room enlarged 2.5 ft. circumferentially at 2 years, and finally the enlarged room with the liner installed 1 month later. As shown, enlarging the room significantly increases the displacement (almost doubled at 12 years) and displacement rates of the rock. This suggests that enlarging should be kept to a minimum. Also shown is the effectiveness of the liner in reducing rock deformations. The desirability of installing the liner as soon as possible after enlarging the room is emphasized.

#### 4.4 Conclusions

The sensitivity of the backpressure exerted on the rock, the maximum liner hoop stress, and rock displacements due to changes in liner thickness, concrete properties, and liner emplacement times were evaluated.

Changes in the liner modulus over its practical working range (21.5 to 37.3 GPa) resulted in little change in backpressure, hoop stresses, and rock displacements. Most significant was the increase in concrete strength associated with the increase in modulus. This can result in a change from an unstable to a stable 2.5 ft. thick liner installed 1 month after mining.

Backpressure and hoop stress showed a relative lack of sensitivity to post-mining liner emplacement times. The backpressure and hoop stresses significantly rose when the liner accepted the elastic deformations of the room due to its mining. To model this condition, the liner was simulated as being emplaced prior to mining. In reality, this condition could be approached only if the liner were installed at the mining face and allowed to harden before further mining of the room. Rock displacements were essentially halted by the installation of the liners at all emplacement times. The desirability of installing a liner early is emphasized because of the relatively rapid increase in room closure at early times.

Liner thickness showed a moderate sensitivity to backpressure, hoop stress, and rock displacements. The sensitivity was moderated once liner thickness reached approximately 2.5 ft. The thickness of the liner should be limited because larger liners require more excavation and consequentially larger rock displacements. On the other hand, a very thin liner does not as effectively reduce displacements, and liner stresses were predicted to exceed the compressive strength of the concrete. These competing effects suggest that the desirable liner thickness may be approximately 2.5 ft. thick.

In conclusion, a 2.5 ft. thick circular concrete liner with a compressive strength of at least 6000 psi installed as early as possible after mining of the room appears to be a reasonable design for conceptual purposes. However, if the additional benefit of special liner emplacement techniques are employed (e.g., emplacing as close to the face as possible), the liner compressive strength needs to be significantly increased. A higher strength concrete and/or steel supports added to the liner would help alleviate the potential overstress associated with such emplacement techniques. Thickening the liner may not be an acceptable alternative in reducing the hoop stresses to an acceptable level as rock displacements significantly increase with enlarging of the room.

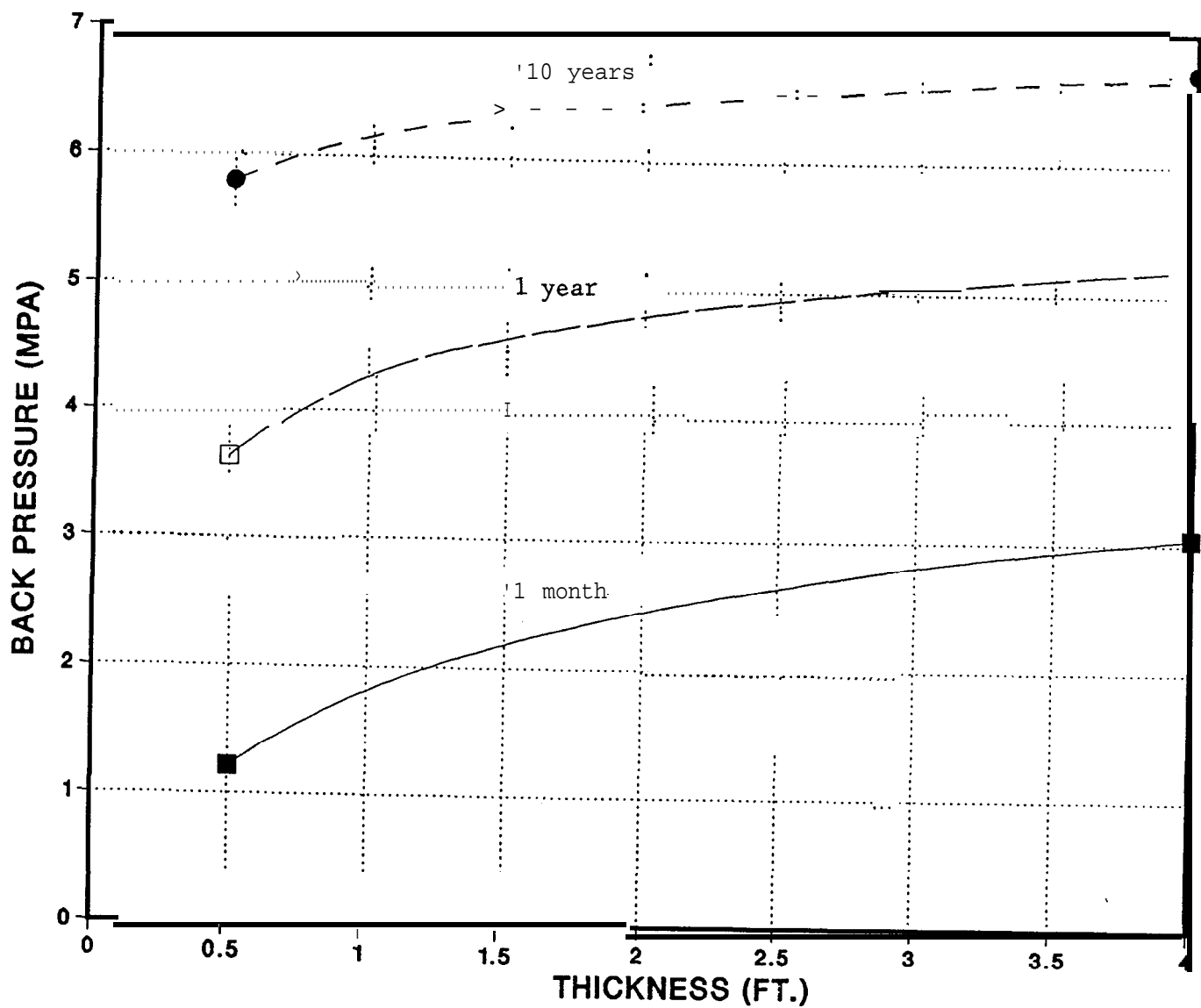


Figure 7. Backpressure Exerted on Rock at 1 Month, 1 Year, and 10 Years After Emplacement of Circular Liner. Liners of various thickness were emplaced 1 month after excavation of the room.

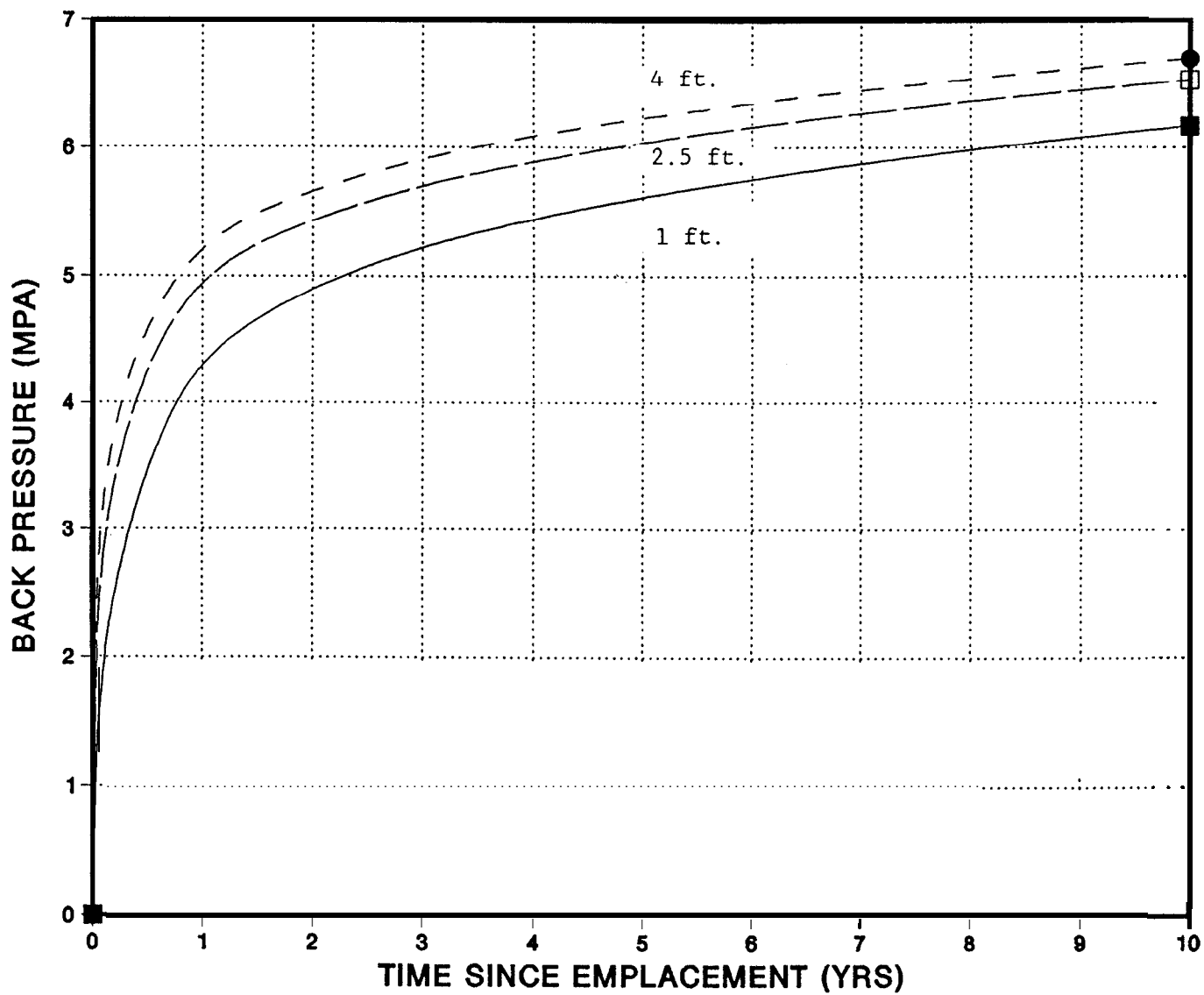


Figure 8. Backpressure Exerted on Rock For 1, 2.5, and 4 Ft. Thick Circular Liners. Liners were emplaced 1 month after excavation of the room.

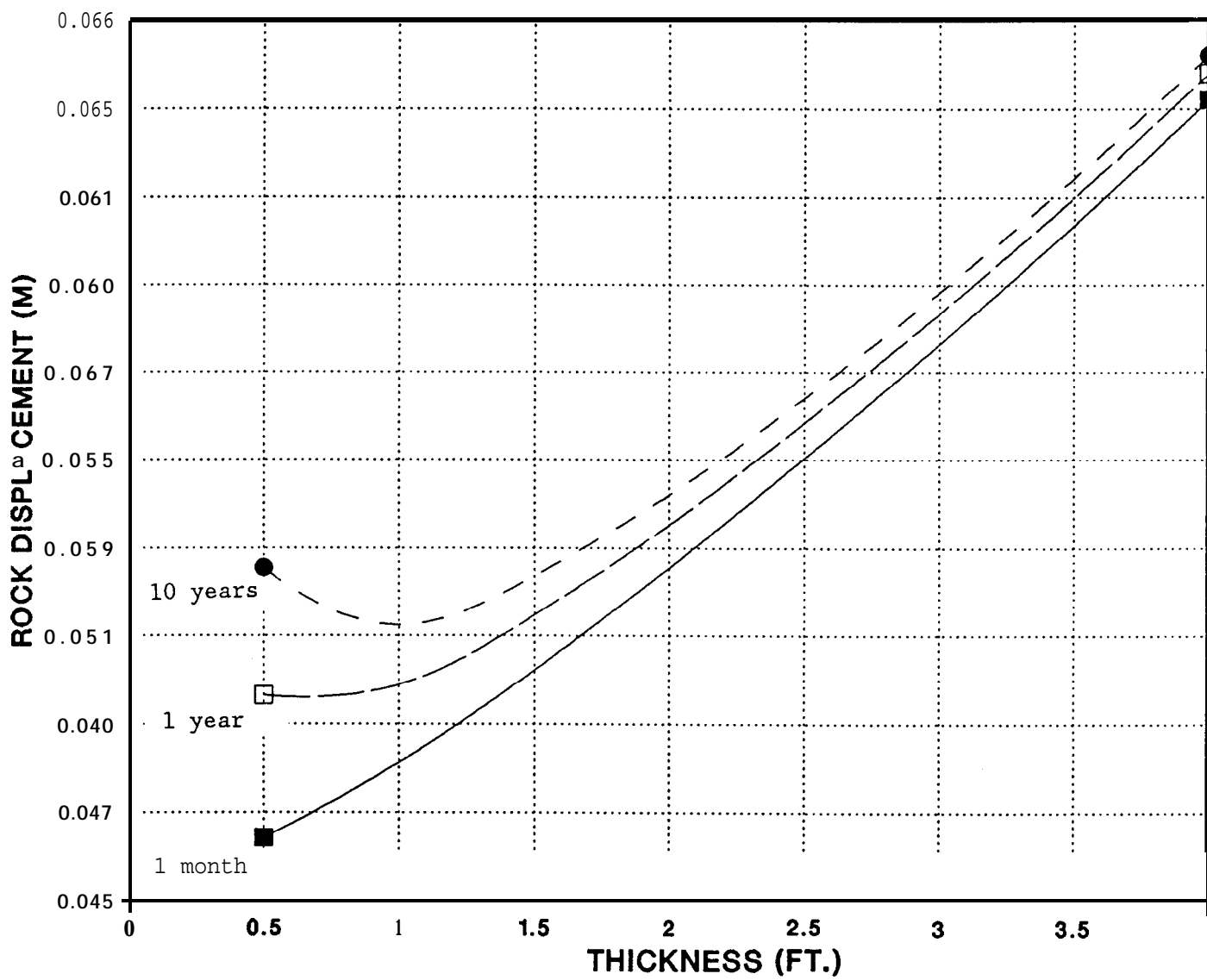


Figure 9. Radial Rock Displacements at 1 Month, 1 Year, and 10 Years After Emplacement of Circular Liner. Liners of various thickness were emplaced 1 month after excavation of the room.

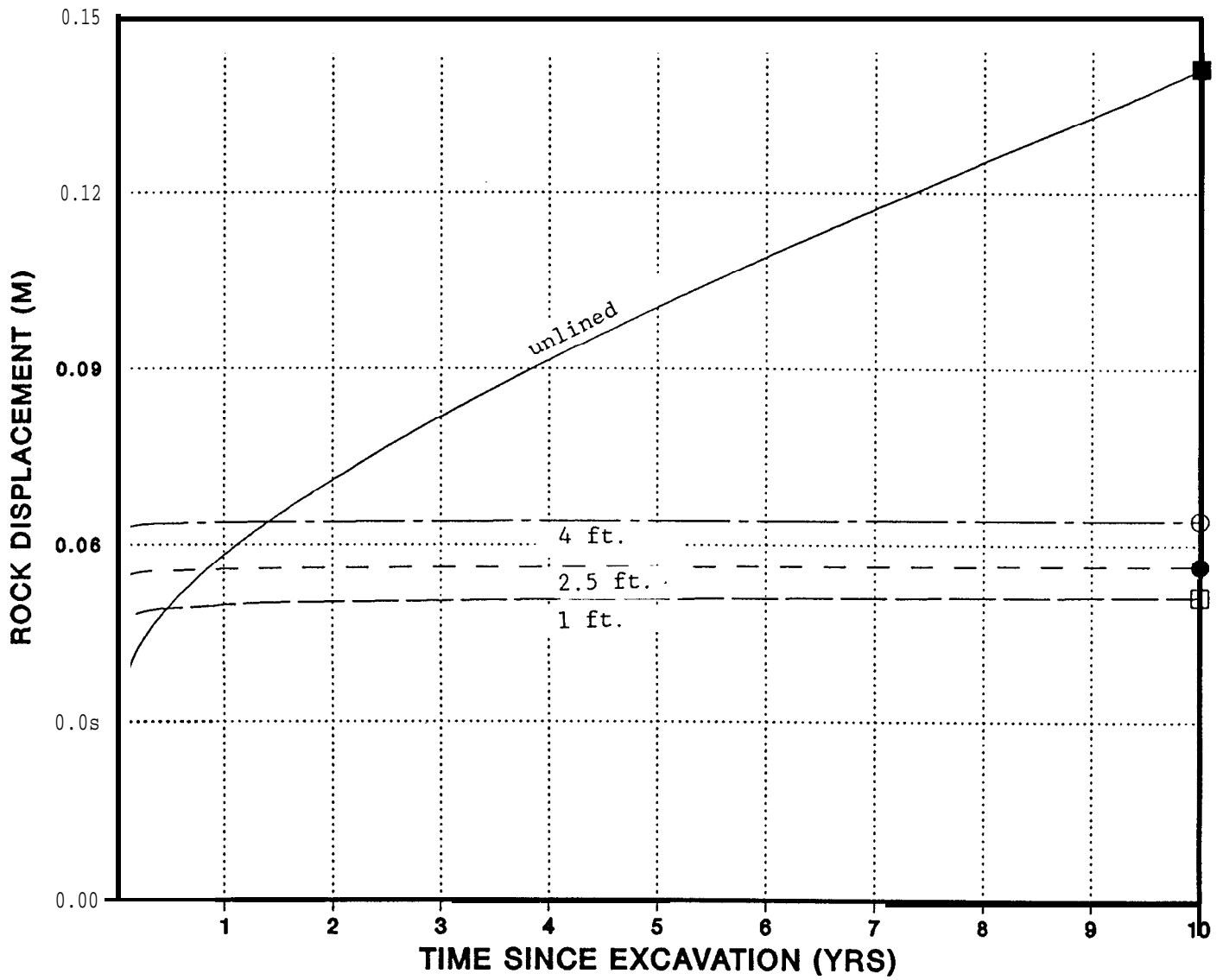


Figure 10. Radial Rock Displacement Histories for 1, 2.5, and 4 Ft. Thick Circular Liners. Also shown is 16 ft. diameter room containing no Liners. Liners were emplaced 1 month after excavation of the room.

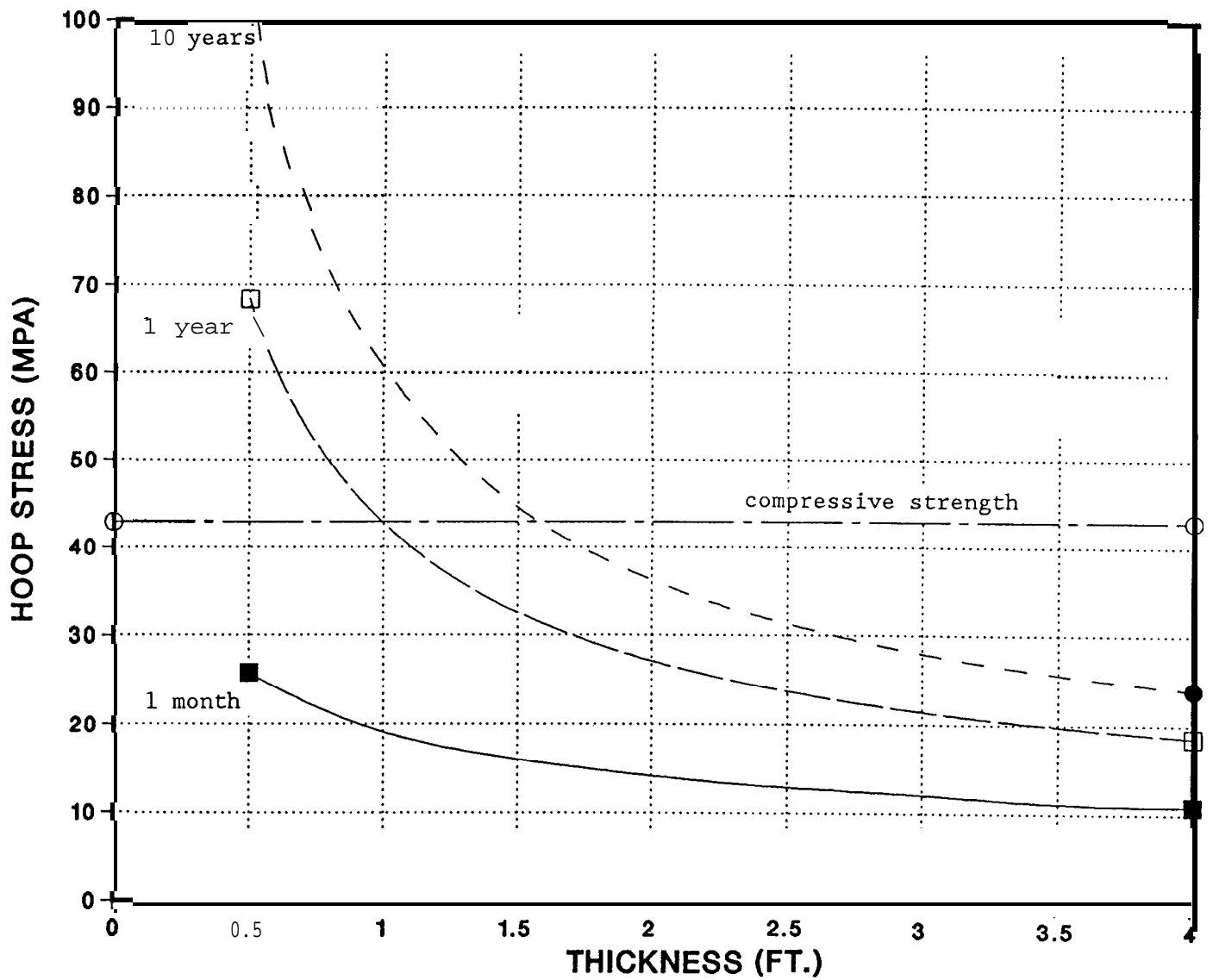


Figure 11. Maximum Hoop Stresses in Circular Liner at 1 Month, 1 Year, and 10 Years After Emplacement of Liner. Liners of various thickness were emplaced 1 month after excavation of the room.

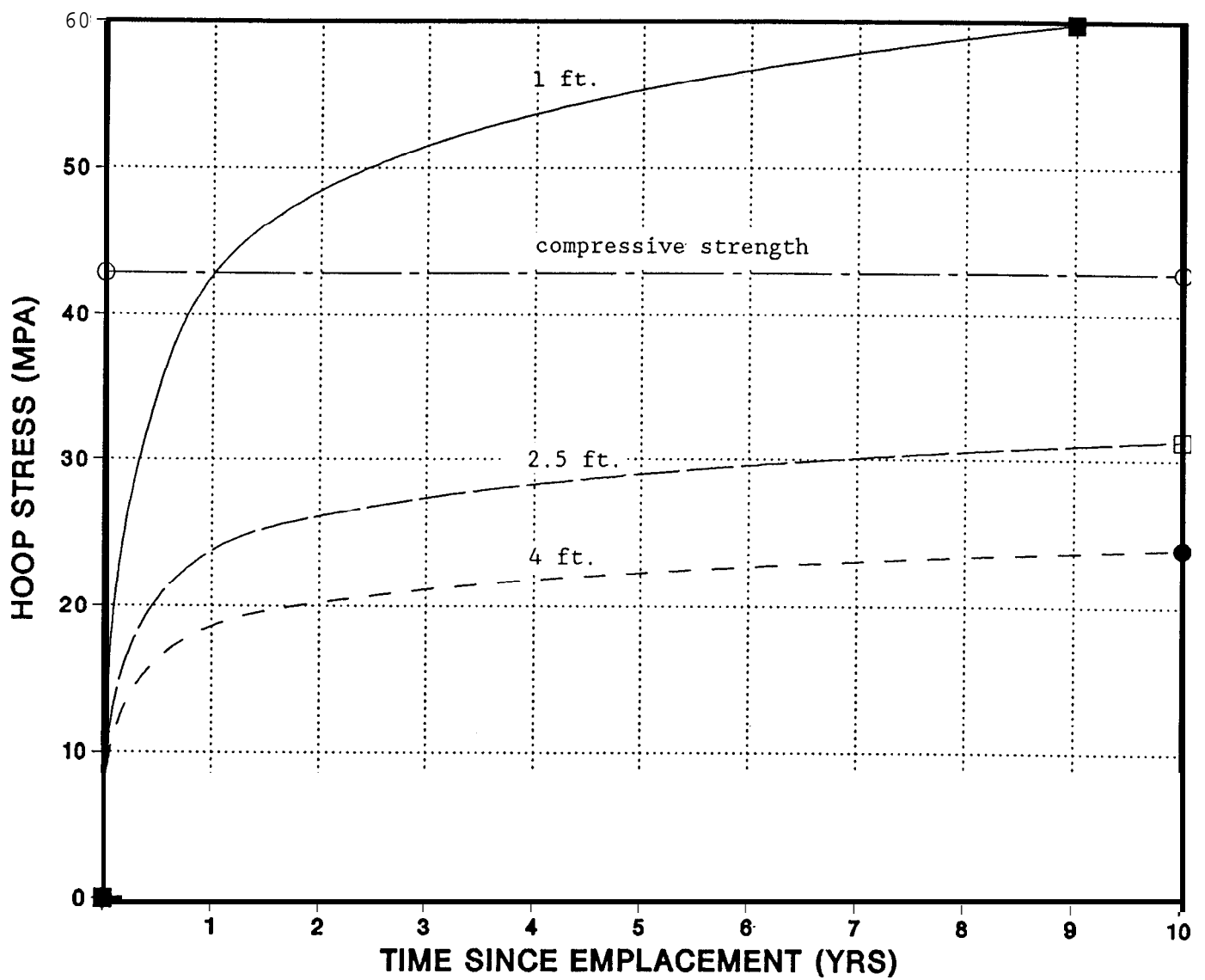


Figure 12. Maximum Hoop Stresses in Circular Liner for 1, 2.5, and 4 Ft. Thick Liners. Liners were emplaced 1 month after excavation of the room.

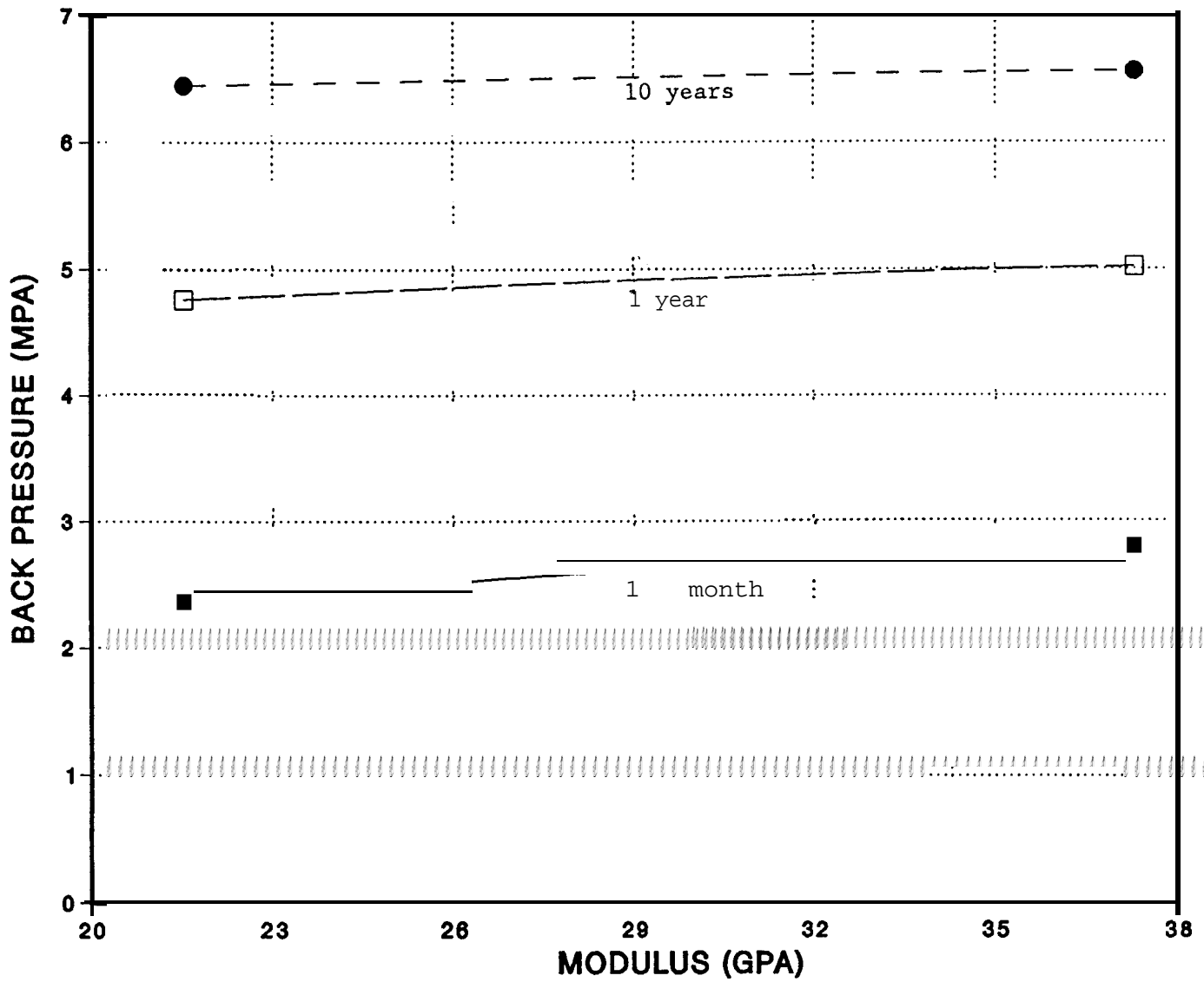


Figure 13. Backpressure Exerted on Rock at 1 Month, 1 Year, and 10 Years After Emplacement of a 2.5 Ft. Thick Circular Liner. Liners of various concrete moduli (as related to compressive strength) were emplaced 1 month after excavation of the room.

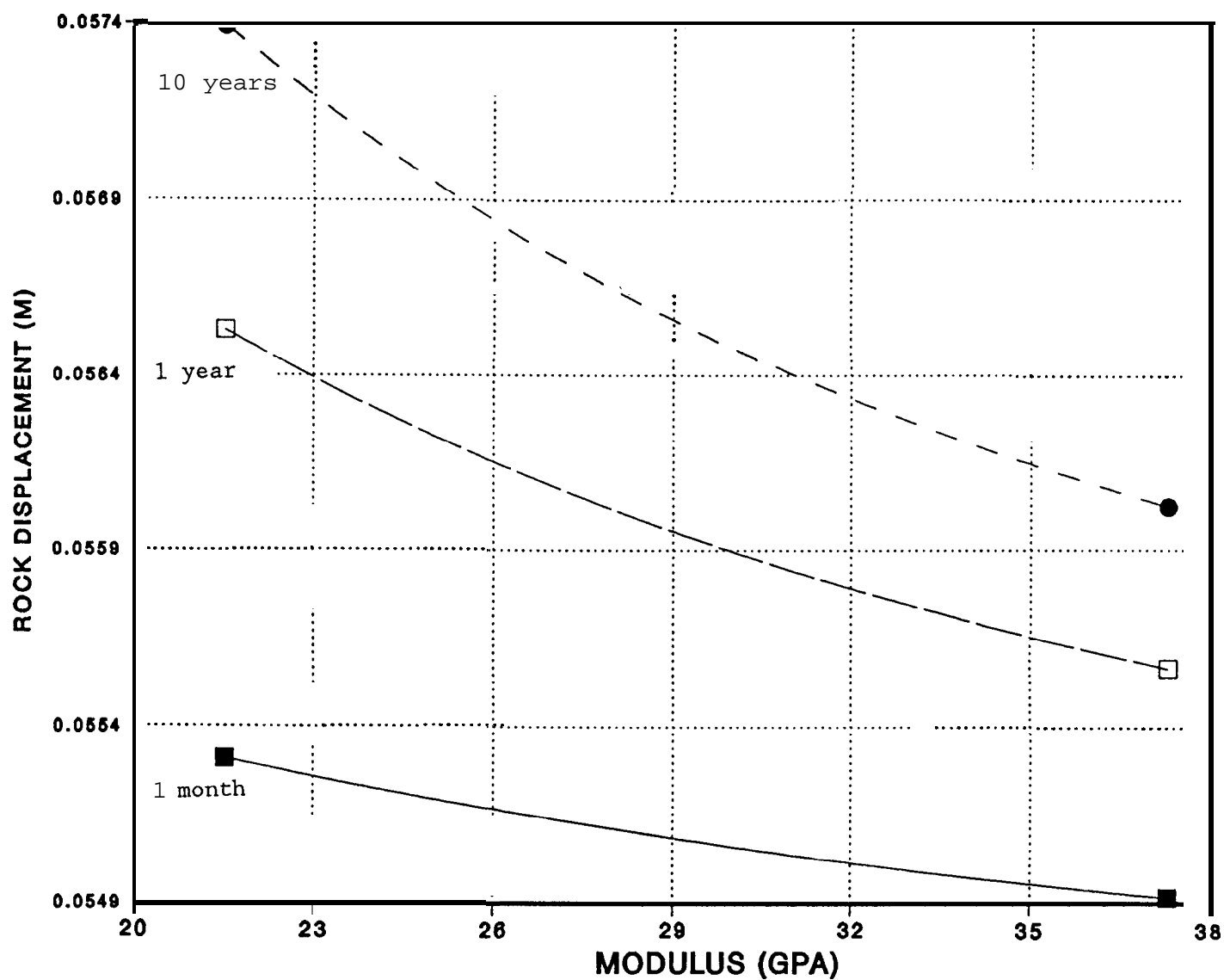


Figure 14. Radial Rock Displacements at 1 Month, 1 Year, and 10 Years After Emplacement of a 2.5 Ft. Thick Circular Liner. Liners of various concrete moduli (as related to compressive strength) were emplaced 1 month after excavation of the room.

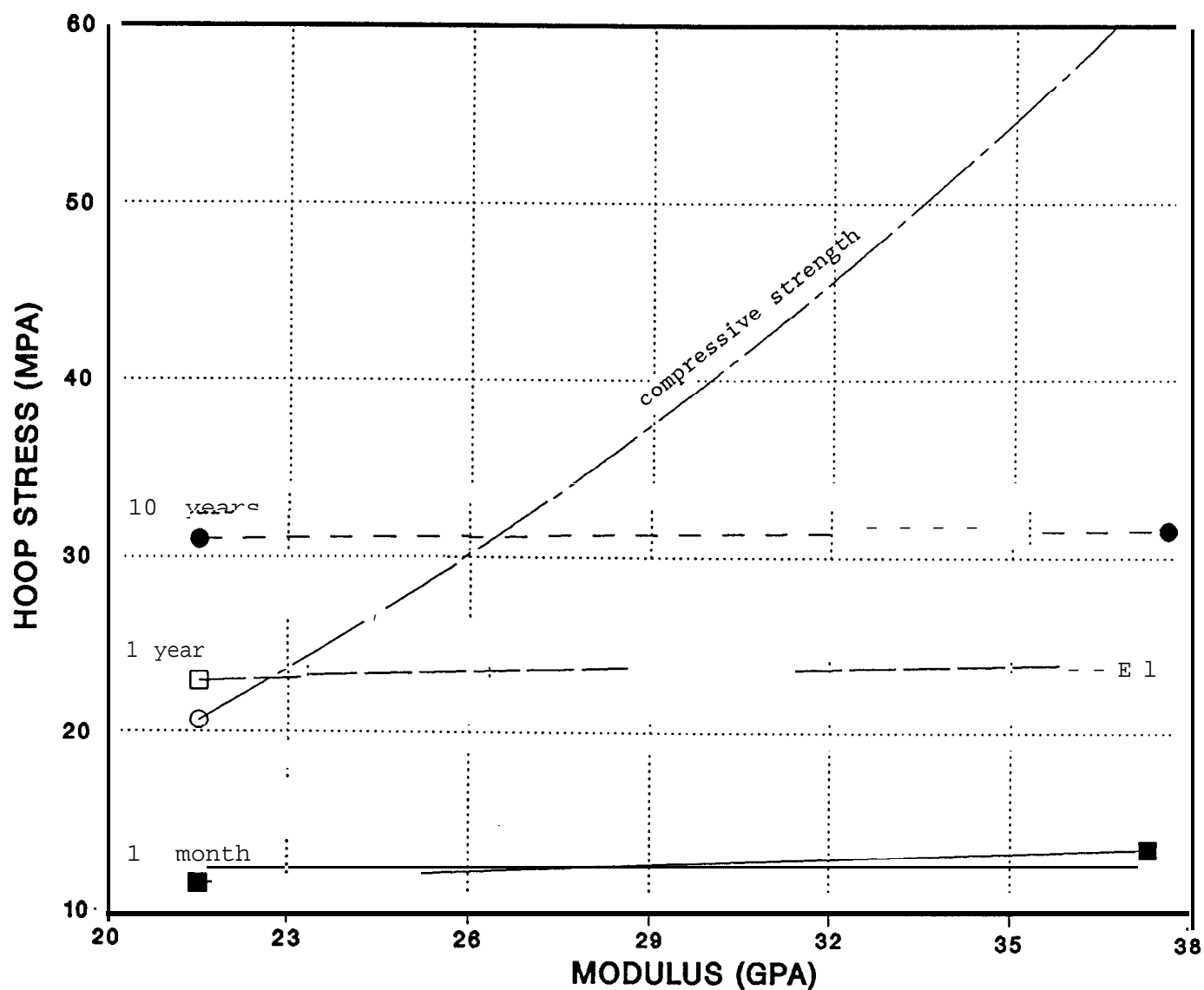


Figure 15. Maximum Hoop Stresses in Liner 1 Month, 1 Year, and 10 Years After Emplacement of a 2.5 Ft. Thick Circular Liner. Liners of various concrete moduli (as related to compressive strength) were emplaced 1 month after excavation of the room.

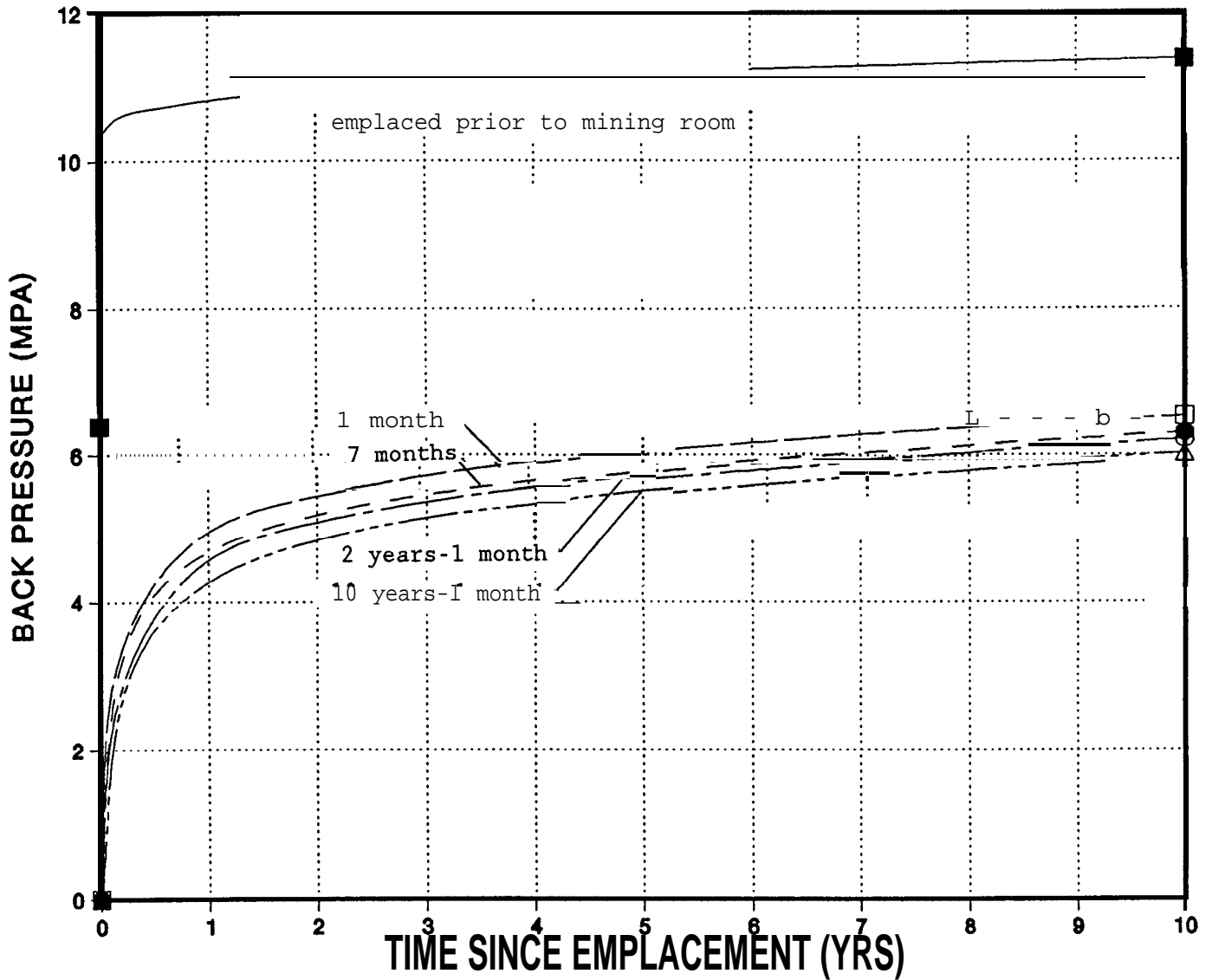


Figure 16. Backpressure Exerted on Rock due to a 2.5 Ft. Thick Circular Liner Emplaced Prior to Room Excavation, and at 1 Month, 7 Months, 2 Years-1 Month, and 10 Years-1 Month Following Excavation. For post mining liner emplacements, room was enlarged 1 month prior to liner emplacement times.

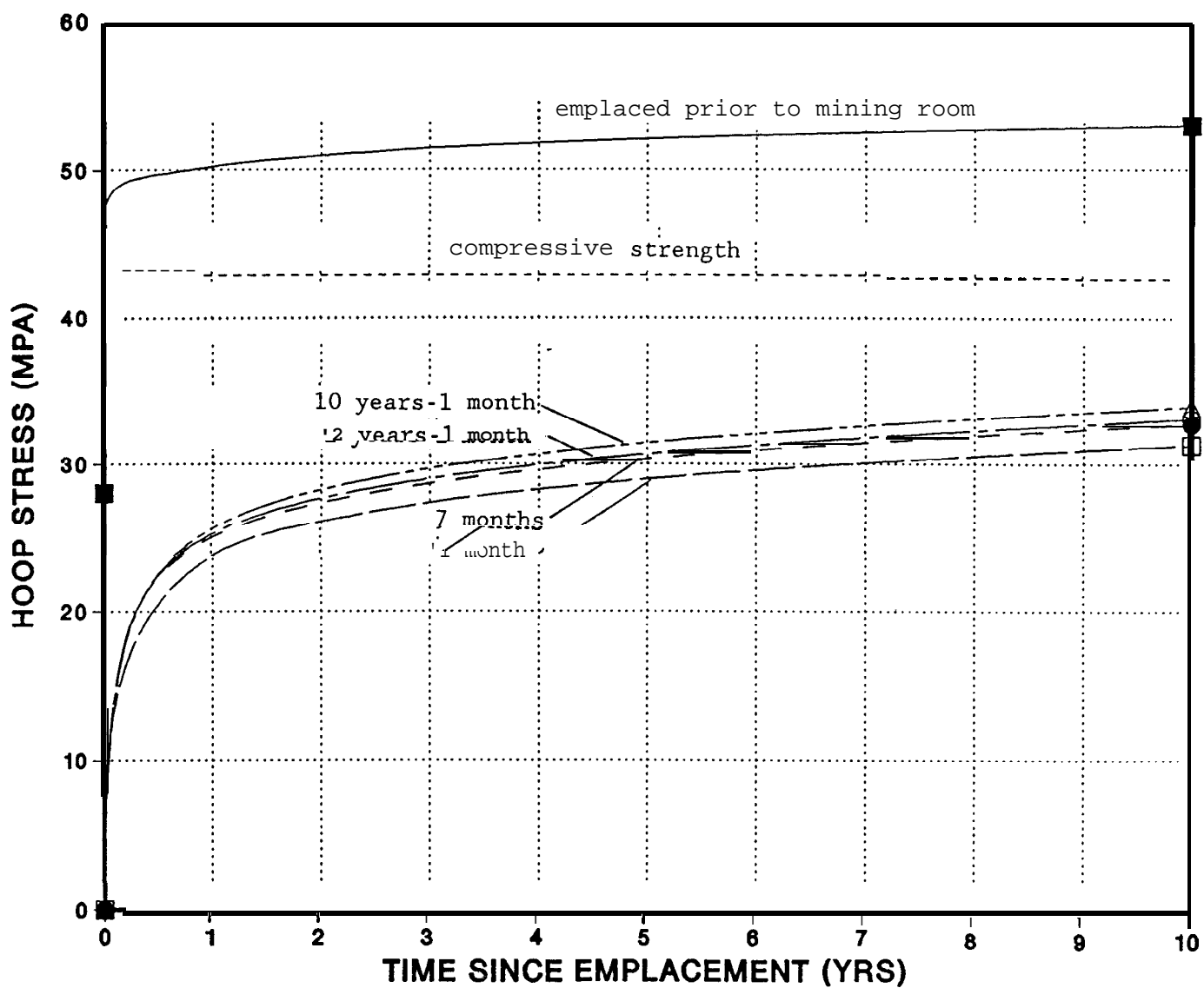


Figure 17. Maximum Hoop Stresses in a 2.5 Ft. Thick Circular Liner Emplaced Prior to Room Excavation, and at 1 Month, 7 Months, 2 Years-1 Month, and 10 Years-1 Month Following Excavation. For post-mining liner emplacements, room was enlarged 1 month prior to liner emplacement times.

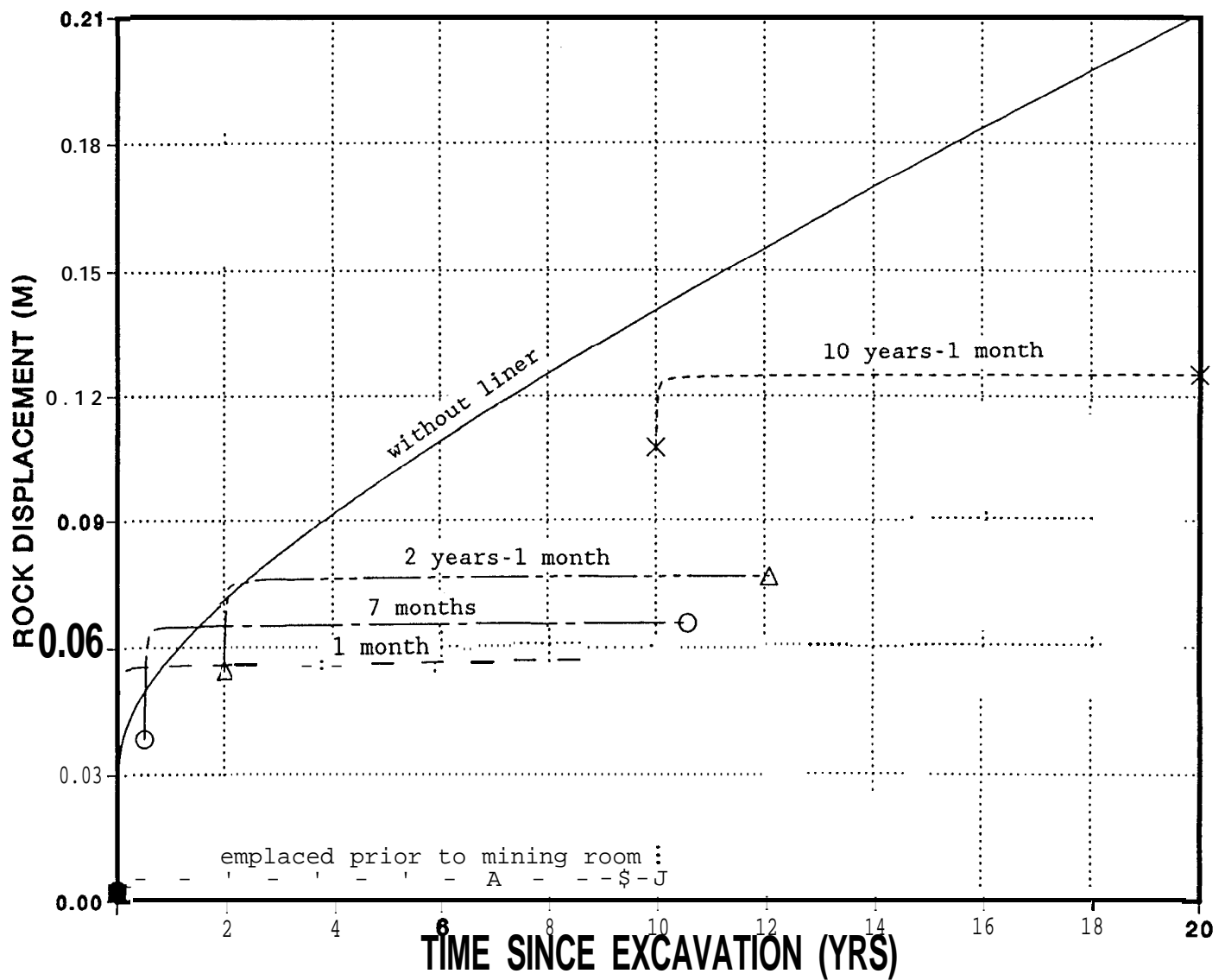


Figure 18. Radial Rock Displacement Histories for a 2.5 ft. Thick Circular Liner Emplaced Prior to Room Excavation, and at 1 Month, 7 Month, 2 Years-1 Month, and 10 Years-1 Month Following Excavation. Also shown is the displacement history of a 16 ft. diameter room containing no liner. For post-mining liner emplacements, room was enlarged 1 month prior to liner emplacement times.

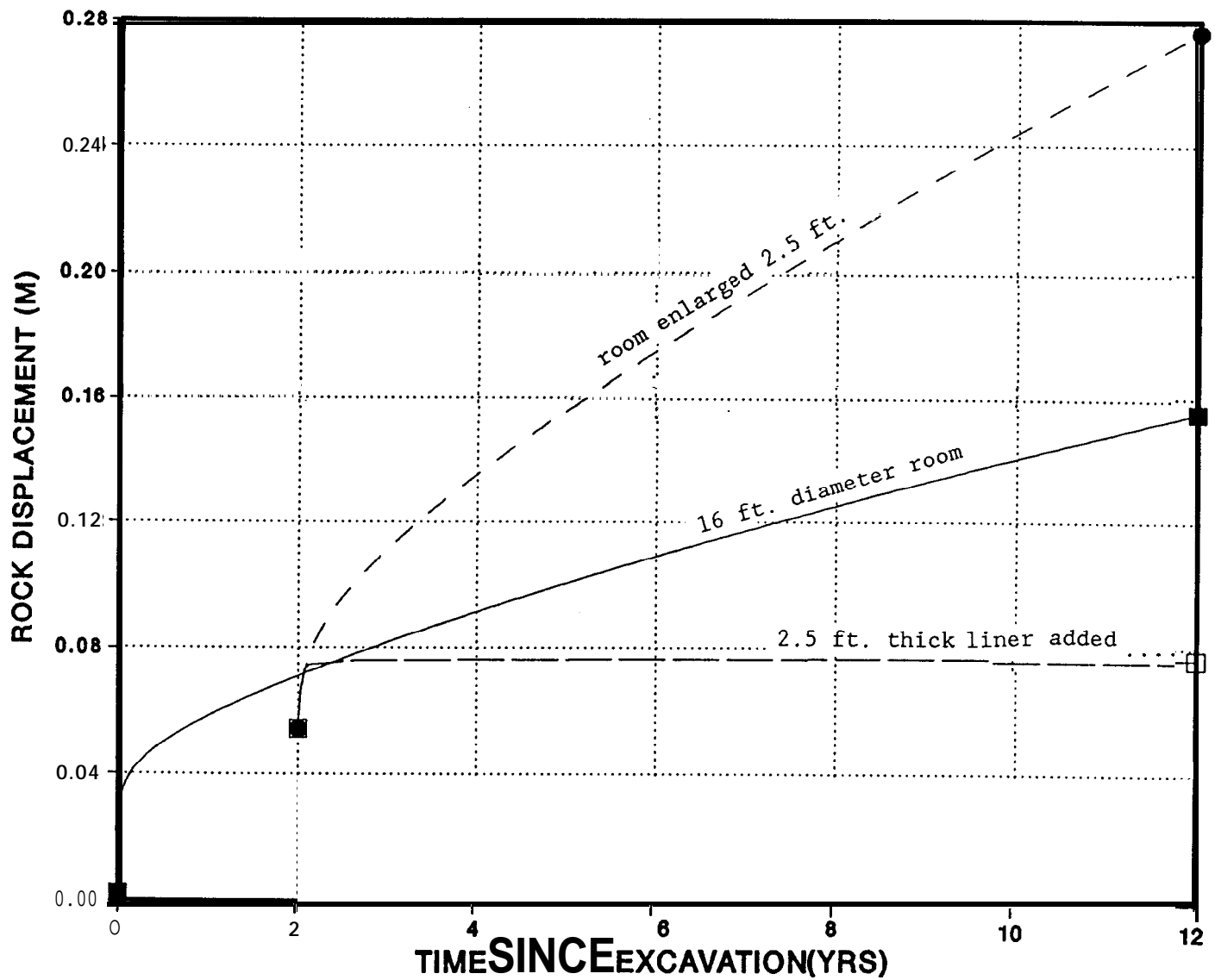


Figure 19. Radial Rock Displacement Histories for 1) a 16 Ft. Diameter Circular Room, 2) the Room Enlarged 2.5 Ft. Circumferentially at 2 Years, and 3) the Enlarged Room with a 2.5 Ft. Thick Liner Emplaced 1 Month Following Enlargement.

## 5.0 ARCH-SHAPED LINER DESIGN

### 5.1 Introduction

These analyses continue the study performed to assess the feasibility of emplacing a concrete liner about the perimeter of a room that would provide backpressure to the host rock and limit rock deformations while the drift is relatively young, yet allow access through the liner for operational purposes. The intent of the liner is to retard the growth of the disturbed rock zone (DRZ) surrounding the room and perhaps to facilitate crack healing or limit the growth of cracks in that area as early as possible after mining of the room.

Chapters 3 and 4 showed that a ring-shaped liner emplaced as early as possible to be the favorable design. The work examined various liner thickness showing a trade-off between stability and performance. Thin liners were not structurally adequate, yet thick liners required more excavation and larger magnitudes of rock deformation resulted. The work suggested a concrete thickness of approximately 2.5 ft. as a desirable compromise for a circular liner. Based on the above results, an **arch-shaped** liner design (Figure 20) with internal dimensions appropriate for the alcove gas-generation test (Molecke, 1990) was proposed. The design also took into consideration mining, concrete placement, and grouting aspects (Ahrens, 1990). Although the design addresses sealing alcoves that could be created to accommodate the gas-generation experiment, the same concepts can be used in designing the drift and panel liners (Nowak, Tillerson, and Torres, 1990) used to isolate waste in the WIPP facility.

The mechanical analyses of the arch-shaped liner predicted the liner stresses, backpressures exerted on the rock, and rock displacement histories over a 10 year period for two designs. The first design is shown in Figure 20. It performed well in limiting rock displacements and building up pressure on the host rock, but the stresses in

the concrete floor on the liner exceeded the strength of the concrete. A second analysis, with the floor thickened by 1.6 feet (to 4.1 feet thick), resolved the problem and decreased rock displacements in the floor.

## 5.2 Model and Properties

The arch-shaped room liner was modeled at a depth of 2135 ft. below the surface. The insitu stress at this depth (repository horizon) is estimated at 14.76 MPa in all principal directions. The concrete liner was emplaced 1 month after the instantaneous excavation of the room to decrease the internal dimensions of the room to 17.5 ft. wide by 14.7 ft. high (Figure 20).

The 2-D plane strain finite-element calculations used the mesh shown in Figure 21. The mesh contains 498 elements and 550 nodes. The first three levels of elements surrounding the room modeled the concrete liner. The remaining elements in the mesh modeled salt, with the exception of the second analysis in which the floor was thickened an additional 1.6 feet. For that analysis, eight additional elements below the bottom of the original liner floor were assigned the properties of concrete 1 month after mining of the excavation.

A vertical stress of 13.99 MPa was applied to the upper boundary of the mesh which was located 5 room widths (or 113 ft.) from the center of the liner. An increasing stress gradient existed throughout the salt to the lower boundary, which is similarly located at 5 room widths from the liner. The right boundary was selected to represent the mid-point between alcoves spaced at 133 ft. center to center. This spacing is equivalent to the room spacings in the WIPP panels. The left and right boundaries were modeled as planes of symmetry by confining the nodes to only vertical motion. Thus, infinitely long rooms and liners located in a dimensionless panel were modeled. However, as planned, only 6 alcoves are needed for the gas-generation experiment.

The Munson-Dawson creep model and salt properties as described in Chapter 2 were used to model the salt. The concrete was modeled as an elastic material using the properties defined in Chapter 2.

### 5.3 Results

The three criteria discussed in Chapter 1 were used to evaluate the adequacy of the liner: (1) the liner should apply a significant backpressure to the salt host rock, (2) the liner should limit host rock deformation, and (3) the liner must be structurally stable. As in the other analyses, the liner is assumed to be elastic, and it undergoes compressive loading due to the creep of the host rock. The results of these analyses show the liner stresses to be compressive at all locations over the 10 years simulated.

The backpressures exerted by the liner on the rock, the rock displacement histories, and liner stresses are discussed first for the originally proposed design (Figure 20) and later compared to the altered design that thickens the floor by an additional 1.6 feet. The thicker floor places the bottom of the concrete near the top of anhydrite Marker Bed 139. As discussed in Chapter 2, the Marker Bed was not modeled in the analyses in this report. Sealing of the Marker Bed may require special attention, since the fractured anhydrite will resist healing and may become a potential flow path. Grouting may prove effective in reducing the permeability of the Marker Bed. Alternatively, the Marker Bed may be removed in the vicinity of the floor in favor of a thicker concrete floor.

Figure 22 shows the backpressure exerted on the host rock versus time at the top, mid-wall, and mid-floor of the room. The roof and wall behave similarly in providing a relatively quick build-up in pressure and reach approximately 7 MPa or nearly 50 % of the insitu lithostatic stress after 10 years. The backpressure provided by the wall is slightly greater than that of the roof because of the additional thickness in the

lower portion of the wall. The floor exhibits the same trends as the roof and wall, but lags in magnitude. The reason for this becomes apparent after examining the displacement histories.

Figure 23 shows the displacement histories at the concrete/rock interface in the roof, wall, and floor with and without the concrete liner emplaced. The figure illustrates the effectiveness of the liner in reducing rock deformations. Because of the geometry and gravity effects, the total deformation of the roof and wall is more than that found in the floor. Total deformations, such as those presented in Figure 23, are relative to the time of excavation. However, relative to the time of liner emplacement, the floor deforms more than the roof and walls. This is due to a beaming action of the floor with the center being uplifted. This results in the lower backpressures noted for the floor in Figure 22. It also has an effect on the stresses predicted in the floor of the liner.

Figure 24 plots the maximum compressive stress predicted in the roof, wall, and floor areas of the liner along with the compressive strength of the concrete. The compressive strength represents the unconfined strength as defined in Chapter 2. Confinement adds to the strength of concrete. The maximum stresses in the roof and floor are located along the outside boundaries (nearest the rock) of the concrete, whereas the maximum stress in the wall is located along the inside boundary of the liner. Because the outside boundaries of the liner are in contact with salt, a confinement exists (one component of which is the backpressure) that would serve to increase the compressive strength of the concrete. However, to be conservative, no credit is taken in these preliminary calculations for enhancing the strength of the concrete under these conditions. The figure shows that the floor stresses exceed the compressive strength after the liner is emplaced for approximately 1.5 years. This is a result of the bending action in the floor that increases the compressive stresses along one side of the floor and decreases it along the other. Note that the liner stresses do not become tensile over the time period analyzed. Tensile stresses were

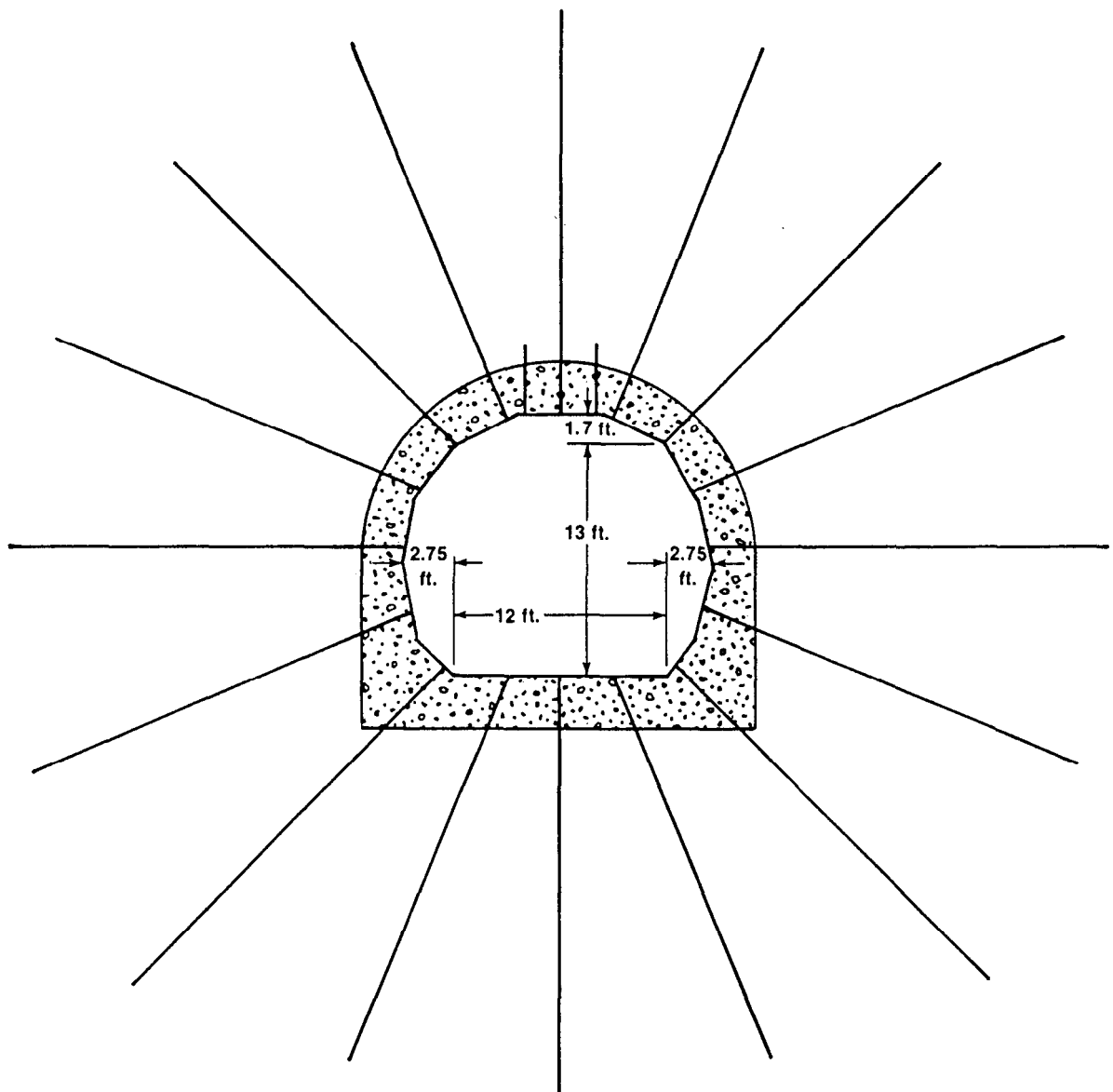
predicted to occur in the 2.5 ft. thick rectangular liner design in Chapter 3. The problem of high compressive stresses was also predicted in the rectangular liner design. The beaming action of the roof, walls, and floor resulted in compressive overstressing of the liner in those areas. To lower the maximum compressive stresses in the floor and improve its overall deformation, the floor of the arch-shaped liner was thickened by 1.6 ft. The results are compared in Figure 25.

Figure 25 shows a significant reduction in maximum compressive stress in the floor when the floor thickness is increased. The stresses in the thickened floor approximate those found in the roof and wall of the liner-- all of which are below the compressive strength of the concrete. Insignificant changes are noted in the backpressures and liner compressive stresses in the wall and roof areas of the liner due to the thickening of the floor. However a significant improvement in backpressure is noted in the floor.

Figure 26 shows the increase in floor backpressure due to the thicker floor. The backpressure is now comparable to those found in the wall and roof areas of the liner (Figure 22).

#### 5.4 Conclusions

The arch-shaped liner design (2.5 ft. thick) is structurally adequate provided that the floor is thickened an additional 1.6 feet. With the thick floor, the maximum compressive stresses predicted at any location in the liner are below the unconfined compressive strength of the concrete. The liner stresses and those exerted on the salt are more uniform as are the rock displacements for the thick floor design. Alternatively, as shown in Chapter 4, the liner could be made structurally adequate if the liner were shaped as a ring, but the circular shape is more difficult to mine with the currently available equipment at the WIPP site.



**ALCOVE  
CROSS SECTION - 3**

0 5 10 ft

Figure 20. Cross-Section of Arch-Shaped Liner Design Showing Liner and Location of Proposed Grout Holes (from Ahrens, 1990). Minimum thickness of concrete is 2.5 ft.

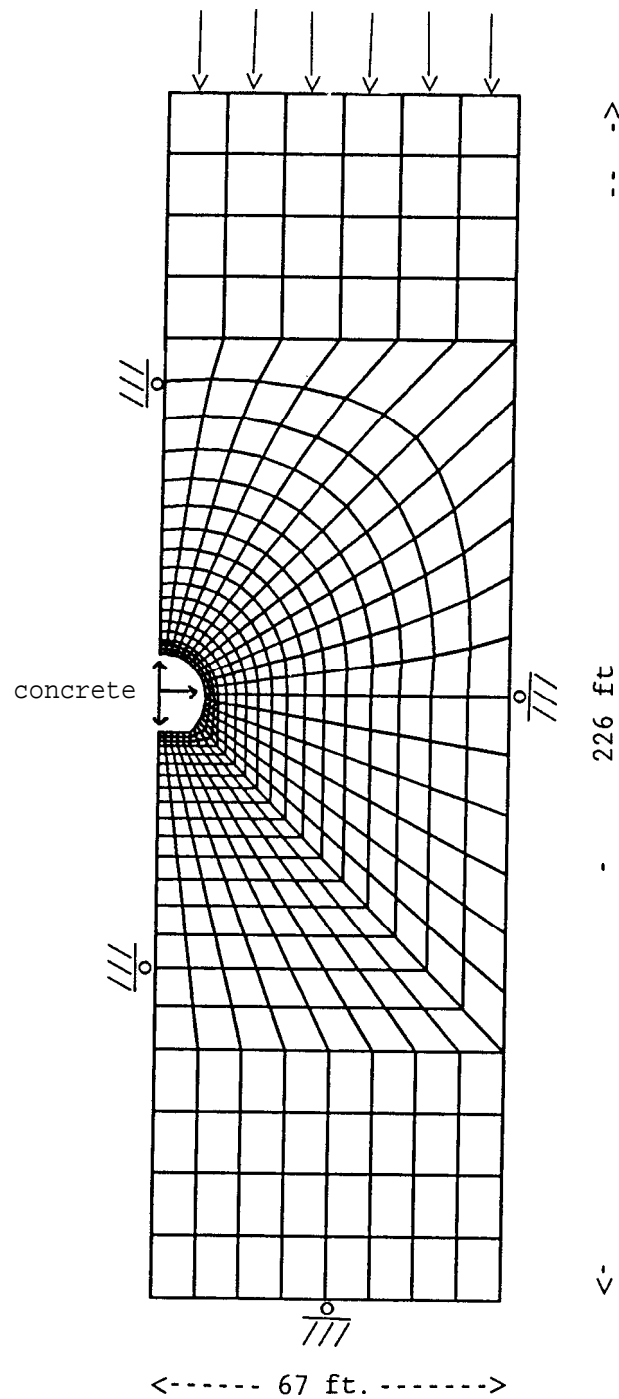


Figure 21. Finite Element Mesh Used to Model Arch-Shaped Liner. Perimeter elements (3 deep) surrounding the room modeled the liner which was emplaced 1 month after the simulated excavation of the room in salt.

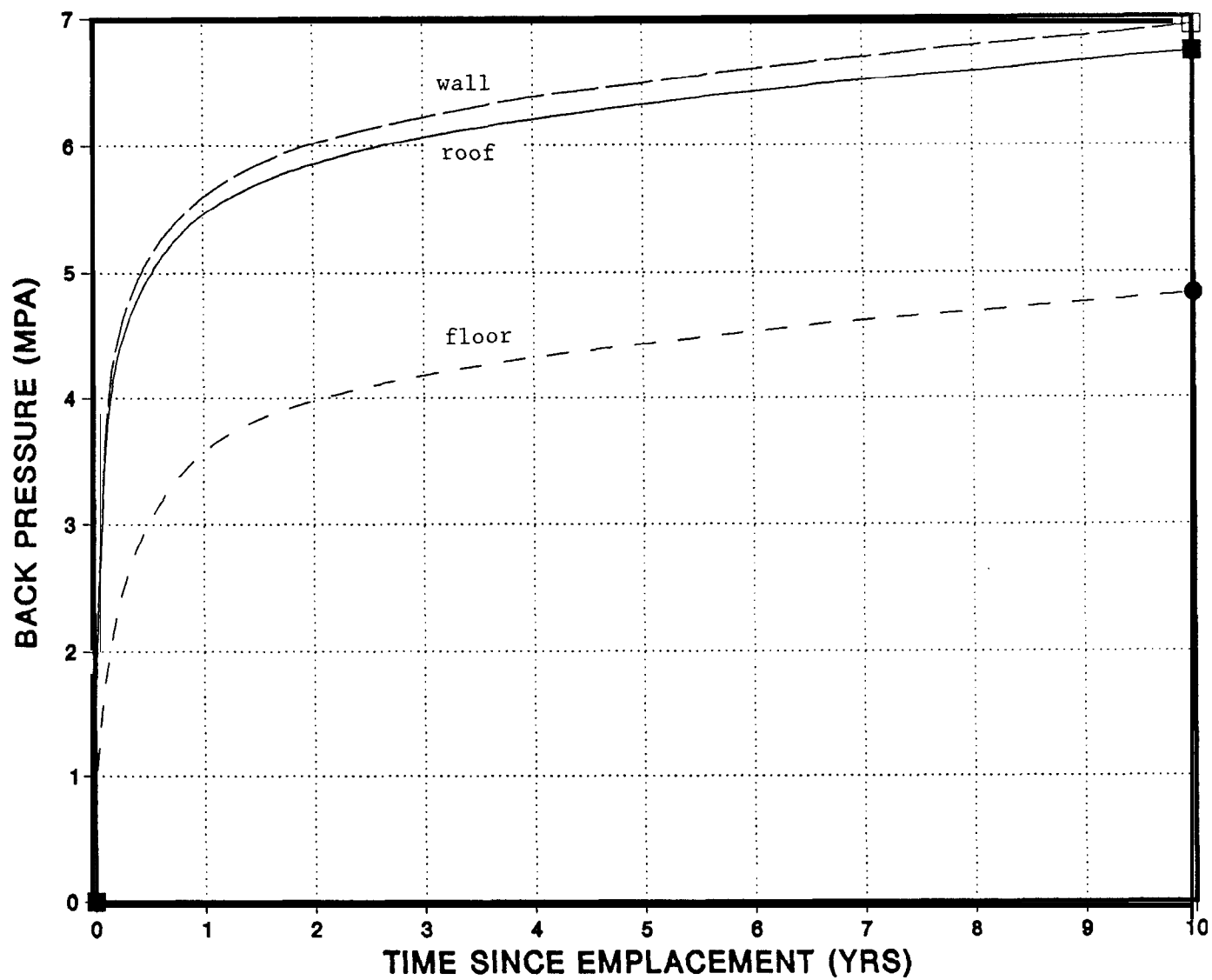


Figure 22. Backpressure Applied to Rock at Roof, Wall, and Floor of Arch-Shaped Liner. Liner was installed 1 month after mining of room.

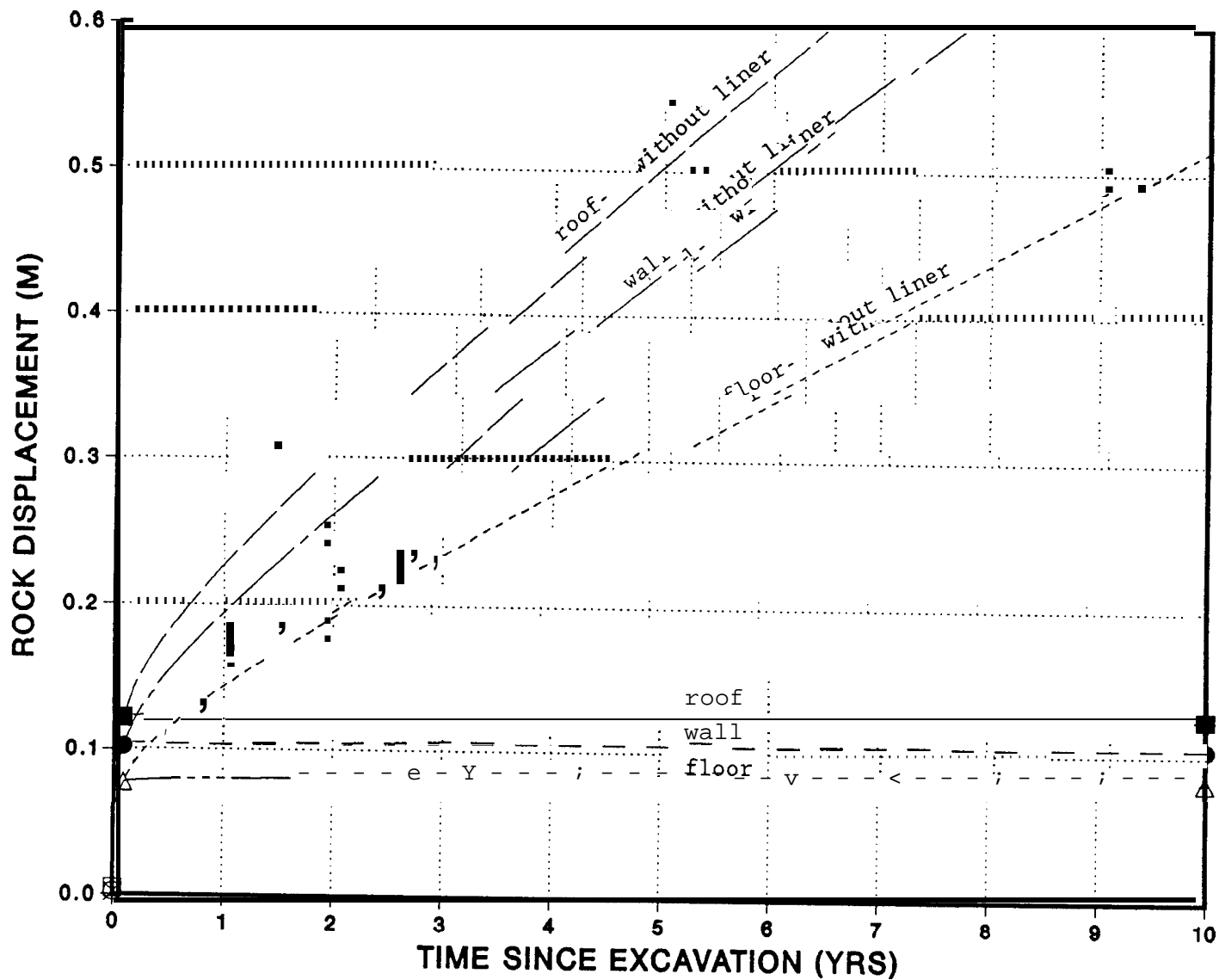


Figure 23. Rock Displacement Histories at Roof, Wall, and Floor of Arch-Shaped Liner. Displacement histories are also shown if no liner were emplaced in the room. Displacements are normal to boundary of room.

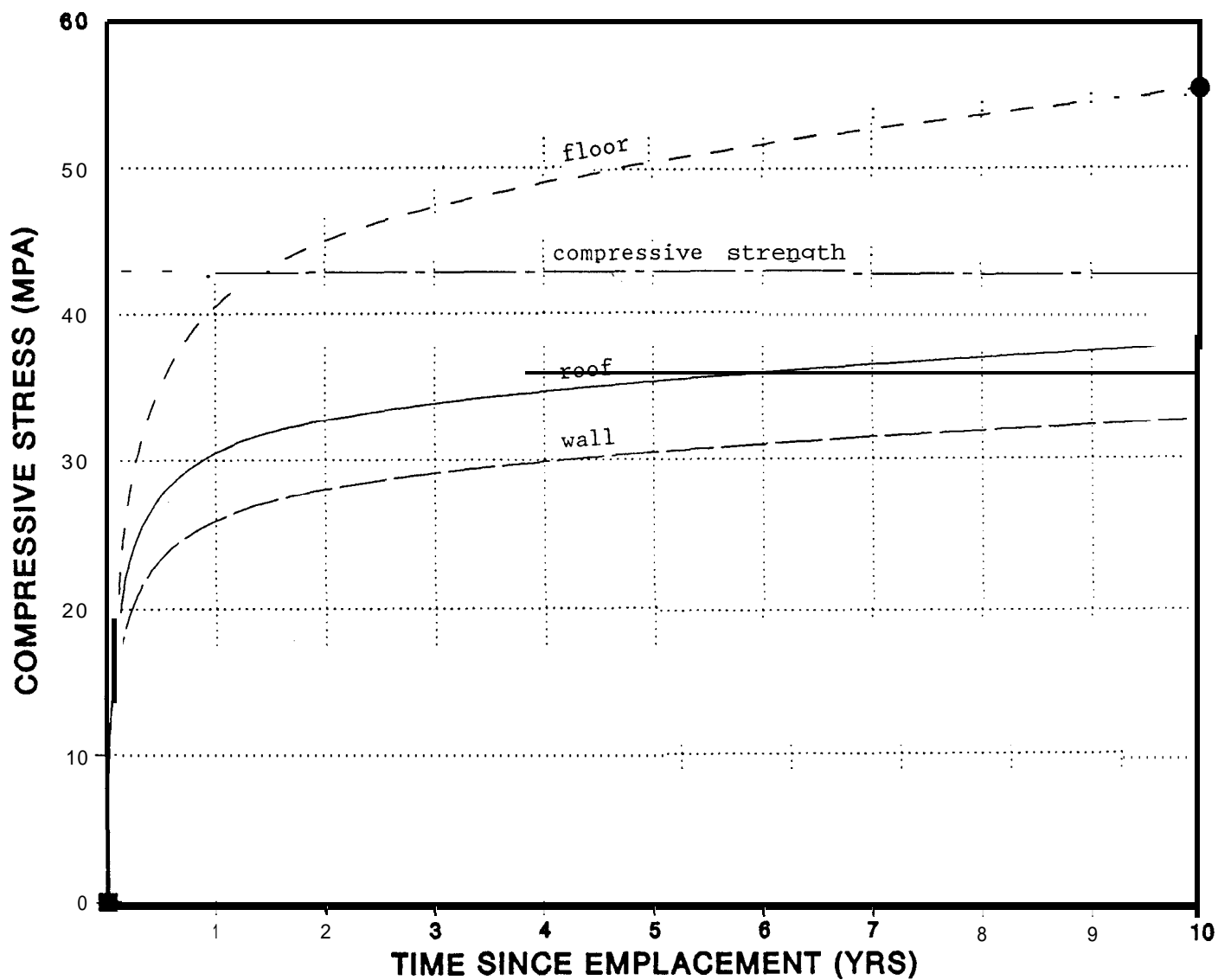


Figure 24. Maximum Compressive Stresses in Roof, Wall, and Floor of Arch-Shaped Liner. Unconfined compressive strength of concrete is also shown.

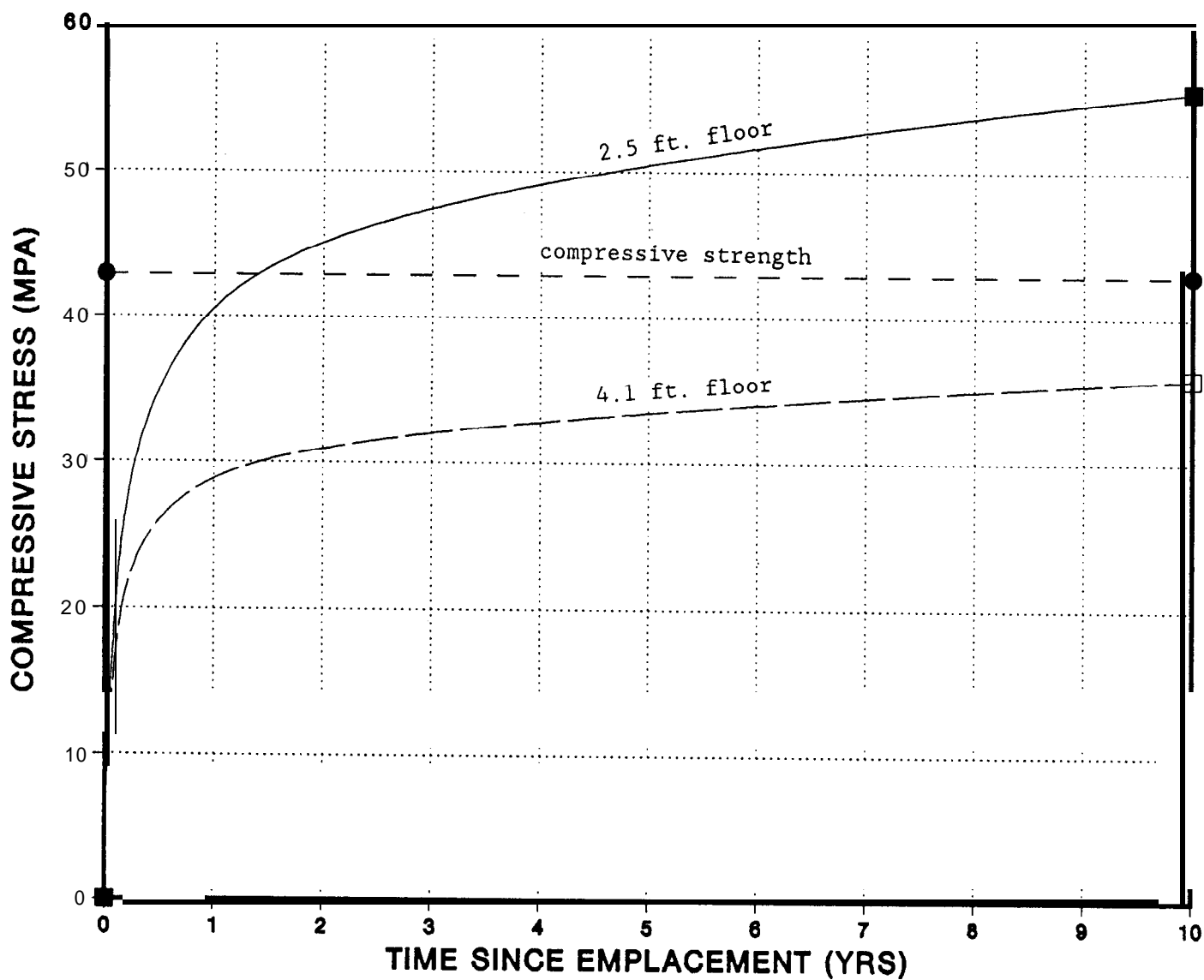


Figure 25. Maximum Compressive Stresses in 2.5 and 4.1 Ft. Thick Arch-Shaped Liner Floors. Unconfined compressive strength of concrete is also shown.

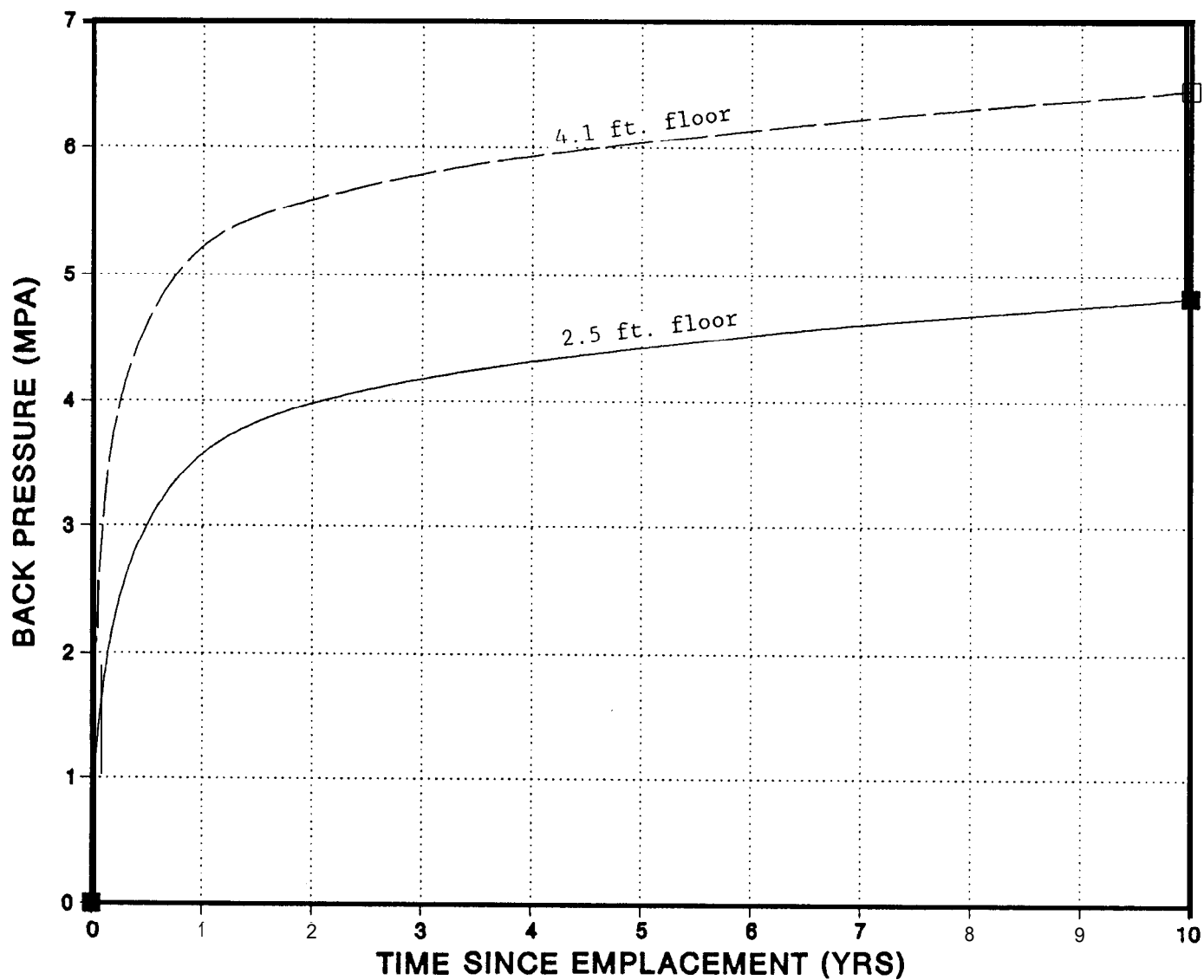


Figure 26. Backpressure Applied to Rock in 2.5 and 4.1 Ft. Thick Arch-Shaped Liner Floors. Liners were installed 1 month after mining of rooms.

## 6.0 CONCLUSIONS

The above analyses demonstrate that a concrete liner can (1) produce significant back pressures on the salt host rock in a relatively short time after its emplacement, (2) essentially halt rock displacements by its emplacement, and (3) can be designed to be mechanically stable. In meeting these three design criteria (defined in Chapter 1), the liner is expected to be effective in mitigating the growth of the DRZ and possibly in healing fractures within the DRZ.

The results show that shape strongly affects the mechanical stability of the liner. The 2.5 ft. thick rectangular concrete liner resulted in excessive localized stress concentrations at the corners of the liner. The walls, floor, and roof suffered from a beam bending mechanism that increased compressive stresses along the outside of the liner and resulted in tensile stresses along the **midspans** of the inside. However, the liner performed sufficiently in exerting backpressure and halting rock displacements. The circular shape liner was considered ideal from a stress point of view where the initial stresses are hydrostatic. However, it is difficult to create such a shape, particularly in the floors, with a roadheader or continuous miner. The circular-shaped liner performed as expected. Liner stresses were significantly reduced in comparison to the rectangular liner of similar thickness and were perfectly uniform. Another shape that evolved was an arch-shaped design. As originally designed it was 2.5 ft. thick. The floor was predicted to be overstressed, but the rest of the liner behaved adequately in meeting the 3 criteria used to evaluate the designs. By thickening the floor an additional 1.6 ft., the floor stresses were reduced and the design was found suitable.

The results show the desirability of installing the liner as soon as possible after the mining of the room or any enlargement made to accommodate the liner. Rock displacement rates, which are highest immediately after excavation, can be significantly reduced upon installation of the liner. In an extreme case, where the liner is

emplaced as part of the mining of the room (see Chapter 5), the elastic relaxation of the rock is initially imposed on the liner. This modeling approach resulted in overstressing of the liner. If this approach were taken, a stronger liner material or perhaps a thicker liner would be required. The benefit of such an approach is reducing the DRZ to the smallest possible size and aperture growth.

The results show that room and liner stresses and the response of the host rock are not significantly affected by changes in concrete modulus. However, since concrete is much stronger for higher moduli mixtures, a high modulus formulation appears desirable.

The results show that liner thickness tends to increase rock displacements as a result of the larger room size required to accommodate the thicker liners. However, thin liners suffer from high hoop stresses and relatively low backpressures. A trade-off study is required to size the liner. The results of these preliminary analyses suggest that the desirable liner thickness is approximately 2.5 ft. thick. This thickness was suitable for both the circular and the **arch**-shaped design with the thicker floor when the liner was emplaced one month after the simulated excavation of the rooms.

Although the above designs address the more immediate concern of sealing 14 ft. wide by 13 ft. high alcoves intended for experimental purposes (Molecke, 1990), the same concepts can be extended to design the drift and panel liners (Nowak, Tillerson, and Torres, 1990) used to isolate waste in the WIPP facility. Caution is urged in extending the results of these calculations to other liner designs because backpressures, rock displacements, and liner stresses are heavily dependent upon liner geometry, liner dimensions, and emplacement time of the liner.

The results of this study are considered preliminary due to its scoping nature. Future evaluations should include the full stratigraphy about the underground rooms. Specifically, Marker Bed 139 needs to be

included in both the design of the liners and in the modeling exercises. Because the Marker Bed is a fractured, noncreeping rock, its removal or extensive grouting may be desired. The liners in this study were simulated as cast-in-place concrete. Alternative liner materials such as steel or the use of pre-cast concrete liners may be considered in future studies. More elaborate constitutive models for concrete might be considered for use in future studies along with potential models of the mechanical behavior of the DRZ. A suitable safety factor for the design needs to be defined and agreed upon prior to final design analyses. The end effects of the liner should be evaluated. Stresses at the open end of the liners will differ from those in the center of the liner. The appropriate length of a liner needs to be defined as well as the design of the ends of the liners. Liner ends may require tapering to avoid fracturing of the salt in those areas. The grout design needs to be developed and more data are needed to quantify the relationship between backpressure and time on permeability of the DRZ. These and other considerations will undoubtedly arise as the design of the liner progresses.

## References

Ahrens, E.H. 1990. Proposed Rigid Seal for the Alcove Room Tests and Thoughts Concerning Effective Sealing of the Interface Between Salt Concrete and Various Materials, internal memo to distribution dated September 17, Sandia National Laboratories, Albuquerque, NM.

Borns, D.J. and J.C. Stormont 1988. An Interim Report on Excavation Effect Studies at the Waste Isolation Pilot Plant: The Delineation of the Disturbed Rock Zone, SAND87-1375, Sandia National Laboratories, Albuquerque, NM.

Krieg, R.D. 1984. Reference Stratigraphy and Rock Properties for the Waste Isolation Plant (WIPP) Project, SAND83-1908, Sandia National Laboratories, Albuquerque, NM.

Molecke, M.A. 1990. WIPP In Situ Alcove CH TRU Waste Tests, -Test Plan, Sandia National Laboratories, Albuquerque, NM.

Munson, D.E. 1979. Preliminary Deformation-Mechanism Map for Salt (with Application to WIPP), SAND70-0076, Sandia National Laboratories, Albuquerque, NM.

Munson, D.E. 1989. Proposed New Structural Reference Stratigraphy, Law, and Properties, Internal technical memorandum to distribution dated August 22, 1989, Sandia National Laboratories, Albuquerque, NM.

Munson, D.E. and P.R. Dawson, 1979. Constitutive Model for the Low Temperature Creep of Salt (with Application to WIPP), SAND79-1853, Sandia National Laboratories, Albuquerque, NM.

Munson, D.E. and K.L. DeVries, 1990. "Progress in Validation of Structural Codes for Radioactive Waste Repository Applications in Bedded Salt," **Proc. of Geoval 90**, Conference sponsored by SKI & OECD/NEA, Stockholm, Sweden.

Munson, D.E., A.F. Fossum, and P.E. Senseny, 1989a. Advances in Resolution of Discrepancies Between Predicted and Measured In Situ WIPP Room Closure, SAND88-2948, Sandia National Laboratories, Albuquerque, NM.

Munson, D.E., A.F. Fossum, and P.E. Senseny, 1989b. Approach to First Principles Model Prediction of Measured WIPP In Situ Room Closure in Salt, SAND88-2535, Sandia National Laboratories, Albuquerque, NM.

Nowak, E.J., J.R. Tillerson, and T.M. Torres, 1990. Initial Reference Seal System Design: Waste Isolation Pilot Plant, SAND90-0355, Sandia National Laboratories, Albuquerque, NM.

RE/SPEC 1989. Documentation of SPECTROM-32: A Finite Element Thermomechanical Stress Analysis Program, RE/SPEC Inc., Rapid City, S.D.

Senseny, P.E. 1990. Creep of Salt from the ERDA-9 Borehole and the WIPP Workings, SAND89-7098, Sandia National Laboratories, Albuquerque, NM.

Thorton, C.H. and Lew, I.P. 1983. "Concrete Design and Construction," Section 8 in Standard Handbook for Civil Engineers, 3rd ed., McGraw-Hill, NY.

## DISTRIBUTION LIST

FEDERAL AGENCIES

U. S. Department of Energy, (5)  
Office of Civilian Radioactive Waste  
Management  
Attn: Deputy Director, RW-2  
Associate Director, RW-10  
Office of Program Administration  
and Resources Management  
Associate Director, RW-20  
Office of Facilities Siting  
and Development  
Associate Director, RW-30  
Office of Systems Integration  
and Regulations  
Associate Director, RW-40  
Office of External Relations  
and Policy  
Forrestal Building  
Washington, DC 20585

U. S. Department of Energy (3)  
Albuquerque Operations Office  
Attn: J. E. **Bickel**  
R. Marques, Director  
Public Affairs Division  
P.O. Box 5400  
Albuquerque, NM 87185

U. S. Department of Energy  
Attn: National Atomic Museum Library  
Albuquerque Operations Office  
P. O. Box 5400  
Albuquerque, NM 87185

U. S. Department of Energy (4)  
WIPP Project Office (**Carlsbad**)  
Attn: Vernon Daub  
J.A. Mewhinney  
P.O. Box 3090  
Carlsbad, NM 88221

U. S. Department of Energy  
Research & Waste Management Division  
Attn: Director  
P. O. Box E  
Oak Ridge, TN 37831

U.S. Geological Survey  
Branch of Regional Geology  
Attn: R. Snyder  
MS913, Box 25046  
Denver Federal Center  
Denver, CO 80225

U.S. Nuclear Regulatory **Commission** (4)  
Division of Waste Management  
Attn: J. Bunting HLEN **4H3 OWFN**  
R. Ballard HLGP **4H3 OWFN**  
Jacob Philip  
NRC Library  
Mail Stop **623SS**  
Washington, DC 2055

U.S. Department of Energy  
Waste Management Division  
Attn: R. **F. Guercia**  
P.O. Box 550  
Richland, WA 99352

U. S. Department of Energy (2)  
Idaho Operations Office  
Fuel Processing and Waste  
Management Division  
785 DOE Place  
Idaho Falls, ID 83402

U.S. Department of Energy  
Savannah River Operations Office  
Defense Waste Processing  
Facility Project Office  
Attn: W. D. Pearson  
P.O. Box A  
Aiken, SC 29802

U.S. Department of Energy (1)  
Attn: Edward Young  
Room E-178  
**GAO/RCED/GTN**  
Washington, DC 20545

U.S. Department of Energy (6)  
Office of Environmental Restoration and Waste  
Management  
Attn: Jill **Lytle**, EM-30  
Mark **Frei**, EM-34 (3)  
Mark Duff, EM-34  
Clyde Frank EM-50  
Washington, DC 20585

U.S. Department of Energy  
Office of Environment, Safety and Health  
Attn: Ray Pelletier, EH-231  
Kathleen **Taimi**, EH-232  
Carol Borgstrom, EH-25  
Washington, DC 20585

U.S. Environmental Protection Agency (2)  
Attn: Ray Clark  
Office of Radiation Programs (ANR-460)  
Washington, DC 20460

U.S. Geological Survey (2)  
Water Resources Division  
Attn: Kathy Peter  
Suite 200  
4501 Indian School, NE  
Albuquerque, NM 87110

U.S. Geological Survey  
Conservation Division  
Attn: W. Melton  
P.O. Box 1857  
**Roswell**, NM 88201

#### BOARDS

Defense Nuclear Facilities Safety Board  
Attn: **Dermont Winters**  
Suite 700  
625 Indiana Ave., NW  
Washington, DC 20004

Nuclear Waste Technical Review Board (2)  
Attn: Dr. Don A. Deere  
Dr. Sidney J.S. Parry  
**Suite 910**  
1100 Wilson Blvd.  
Arlington, VA 22209-2297

U.S. Department of Energy  
Advisory Committee on **Nuclear Facilities Safety**  
Attn: Merritt E. **Langston**, AC21  
Washington, DC 20585

Richard Major  
Advisory **Committee** on Nuclear Waste  
Nuclear Regulator **Commission**  
7920 Norfolk Avenue  
Bethesda, MD 20814

#### STATE AGENCIES

Environmental Evaluation Group (3)  
Attn: Librarian  
Suite F-2  
7007 Wyoming Blvd., N.E.  
Albuquerque, NM 87109

New Mexico Bureau of Mines  
and Mineral Resources (2)  
Attn: F. E. Kottolowski, Director  
J. Hawley  
Socorro, NM 87801

NM Department of Energy & Minerals  
Attn: Librarian  
**2040 S. Pacheco**  
Santa Fe, NM 87505

NM Environmental Improvement Division  
Attn: Deputy Director  
1190 St. Francis Drive  
Santa Fe, NM 87503

#### LABORATORIES/CORPORATIONS

Battelle Pacific Northwest Laboratories (6)  
Attn: D. J. Bradley, **K6-24**  
J. Relyea, **H4-54**  
R. E. Westerman, **P8-37**  
H. C. Burkholder, **P7-41**  
L. Pederson, **K6-47**  
Battelle Boulevard  
Richland, WA 99352

Savannah River Laboratory (6)  
Attn: N. Bibler  
E. L. Albenisius  
M. J. Plodinec  
G. G. Wicks  
**C. Jantzen**  
J. A. Stone  
Aiken, SC 29801

**George Dymmel**  
SAIC  
101 Convention Center Dr  
Las Vegas, NV 89109

IT Corporation (2)  
Attn: **D. E. Deal**  
P.O. Box 2078  
Carlshad. NM 88221

Charles R. **Hadlock**  
Arthur D. Little, Inc.  
Acorn Park  
Cambridge, MA 02140-2390

Los **Alamos** Scientific Laboratory  
Attn: B. Erdal, CNC-11  
Los **Alamos**, NM 87545

**RE/SPEC, Inc.**  
Attn: W. Coons  
P. F. Gnirk  
Suite 300  
4775 Indian School Rd., NE  
Albuquerque, NM 87110-3927

**INTERA Technologies, Inc. (4)**

Attn: G. E. **Grisak**  
J. F. **Pickens**  
A. Haug  
A. M. **LeVenue**

Suite **#300**  
6850 Austin Center Blvd.  
Austin, TX 78731

**INTERA Technologies, Inc.**

Attn: Wayne Stensrud  
P.O. Box 2123  
Carlsbad. NM 88221

**IT Corporation (2)**

Attn: R. F. **McKinney**  
J. Myers  
Regional Office - Suite 700  
5301 Central Avenue, NE  
Albuquerque, NM 87108

Science Applications  
International Corporation  
Attn: Michael B. Gross  
Ass't. Vice President

Suite 1250  
160 Spear Street  
San Francisco, CA 94105

**Systems, Science, and Software (2)**

Attn: E. Peterson  
Box 1620  
La Jolla, CA 92038

**RE/SPEC, Inc. (7)**

Attn: L. L. Van **Sambeek**  
G. Callahan  
T. **Pfeifle**  
J. L. Ratigan

P. O. Box 725  
Rapid City, SD 57709

Center for Nuclear Waste  
Regulatory Analysis (4)  
Attn: P.K. Nair  
Southwest Research Institute  
6220 Culebra Road  
San Antonio, TX 78228-0510

Science Applications  
International Corporation  
Attn: Howard R. Pratt,  
Senior Vice President  
10260 Campus Point Drive  
San Diego, CA 92121

**Westinghouse Electric Corporation (7)**

Attn: Library  
Lamar Trego  
W. P. **Poirer**  
W. R. Chiquelin  
V. **F.Likar**  
D. J. **Moak**  
R. F. Kehrman

P. O. Box 2078  
Carlsbad, NM 88221

Weston Corporation  
Attn: David **Lechel**  
**Suite 1000**  
5301 Central Avenue, NE  
Albuquerque, NM 87108

**UNIVERSITIES**

University of Arizona  
Attn: J. G. **McCray**  
Department of Nuclear Engineering  
Tucson, AZ 85721

**University of New Mexico (2)**

Geology Department  
Attn: D. G. **Brookins**  
Library  
Albuquerque, NM 87131

Pennsylvania State University  
Materials Research Laboratory  
Attn: Della Roy  
University Park, PA 16802

Texas **A&M** University  
Center of Tectonophysics  
College Station, TX 77840

G. Ross Heath  
College of Ocean  
and Fishery Sciences  
University of Washington  
Seattle, WA 98195

THE SECRETARY'S BLUE RIBBON PANEL ON WIPP

Dr. Thomas Bahr  
New Mexico State University  
New Mexico Water Resources Institute  
Box 3167  
Las Cruces, NM 88003-3167

Mr. Leonard Slosky  
Slosky & Associates  
Suite 1400  
Bank Western Tower  
1675 Tower  
Denver, CO 80202

Mr. **Newal Squyres**  
Holland & Hart  
P.O. Box 2527  
Boise, Idaho 83701

Dr. Arthur Kubo  
Vice President  
BDM International Inc.  
7915 Jones Branch Drive  
McLean, VA 22102

Mr. Robert Bishop  
Nuclear Management Resources Council  
Suite 300  
1776 I Street, NW  
Washington, DC 20006-2496

INDIVIDUALS

Dennis W. Powers  
Star Route Box 87  
Anthony, TX 79821

LIBRARIES

Thomas **Brannigan** Library  
Attn: Don Dresp, Head Librarian  
106 W. Hadley St.  
Las Cruces, NM 88001

Hobbs Public Library  
Attn: Ms. Marcia Lewis, Librarian  
509 N. Ship Street  
Hobbs, NM 88248

New Mexico State Library  
Attn: **Ms. Ingrid** Vollenhofer  
P.O. Box 1629  
Santa Fe, NM 87503

New Mexico Tech  
Martin Speere Memorial Library  
Campus Street  
**Socorro**, NM 87810

**Pannell** Library  
Attn: Ms. Ruth Hill  
New Mexico Junior College  
Lovington Highway  
Hobbs, NM 88240

WIPP Public Reading Room  
Attn: Director  
Carlsbad Municipal Library  
101 S. **Halagueno** St.  
Carlsbad, NM 88220

Government Publications Department  
General Library  
University of New Mexico  
Albuquerque, NM 87131

NATIONAL ACADEMY OF SCIENCES. WIPP PANEL

Dr. Charles Fairhurst, Chairman  
Department of Civil and  
Mineral Engineering  
University of Minnesota  
500 Pillsbury Dr. SE  
Minneapolis, MN 55455

Dr. Rodney C. Ewing  
Department of Geology  
University of New Mexico  
200 Yale, NE  
Albuquerque, NM 87131

Dr. John O. Blomeke  
Route 3  
Sandy Shore Drive  
Lenoir City, TN 37771

Dr. John D. Bredehoeft  
Western Region Hydrologist  
Water Resources Division  
U.S. Geological Survey (M/S 439)  
345 Middlefield Road  
Menlo Park, CA 94025

Dr. Karl P. Cohen  
928 N. California Avenue  
Palo Alto, CA 94303

Dr. Fred M. Ernsberger  
250 Old Mill Road  
Pittsburgh, PA 15238

Dr. **D'Arcy** A. Shock  
233 Virginia  
**Ponca** City, OK 74601

Dr. Christopher G. Whipple  
Clement International  
Suite 1380  
160 Spear Street  
San Francisco, CA 94105

Dr. Geraldine **Grube**  
Board on Radioactive Waste Management  
GF456  
2101 Constitution Avenue  
Washington, DC 20418

B. John Garrick  
**Pickard, Lowe & Garrick, Inc.**  
2260 University Drive  
Newport Beach, CA 92660

John W. **Healy**  
51 Grand Canyon Drive  
Los **Alamos**, NM 87544

Leonard F. Konikow  
U.S. Geological Survey  
431 National Center  
**Reston**, VA 22092

Jeremiah **O'Driscoll**  
505 Valley Hill Drive  
Atlanta, GA 30350

Dr. Peter B. Myers, Staff  
Director  
National Academy of Sciences  
**Committee** on Radioactive  
Waste Management  
2101 Constitution Avenue  
Washington, DC 20418

Dr. **Ina Alterman**  
Board on Radioactive Waste  
Management  
GF462  
2101 Constitution Avenue  
Washington, DC 20418

#### FOREIGN ADDRESSES

Studiecentrum Voor Kernenergie  
Centre **D'Energie** Nucleaire  
Attn: Mr. A. **Bonne**  
**SCK/CEN**  
Boeretang 200  
B-2400 Mol  
BELGIUM

Atomic Energy of Canada, Ltd. (2)  
Whiteshell Research Estab.  
Attn: Peter **Haywood**  
John Tait  
Pinewa, Manitoba, CANADA  
ROE 1L0

Dr. D. K. Mukerjee  
Ontario Hydro Research Lab  
800 Kipling Avenue  
Toronto, Ontario, CANADA  
**M8Z 5S4**

Claude Sombret  
Centre **D'Etudes Nucleaires**  
De La **Vallee** Rhone  
**CEN/VALRHO**  
S.D.H.A. BP 171  
30205 **Bagnols-Sur-Ceze**  
FRANCE

Bundesministerium fur Forschung und  
**Technologie**  
Postfach 200 706  
5300 Bonn 2  
FEDERAL REPUBLIC OF GERMANY

Bundesanstalt fur Geowissenschaften  
und Rohstoffe  
Attn: Michael **Langer**  
Postfach 510 153  
3000 **Hannover** 51  
FEDERAL REPUBLIC OF GERMANY

Mr. **Francois** Chenevier, **Director(2)**  
 ANDRA  
 Route du Panorama Robert Schumann  
 B.P. 38  
 92266 Fontenay-aux-Roses Cedex  
 FRANCE

Mr. Jean-Pierre **Olivier**  
 OECD Nuclear Energy Agency  
 Division of Radiation Protection  
 and Waste Management  
 38. Boulevard **Suchet**  
 75016 Paris, FRANCE

Kernforschug **Karlsruhe**  
 Attn: K. D. Closs  
 Postfach 3640  
 7500 Karlsruhe  
 FEDERAL REPUBLIC OF GERMANY

Physikalisch-Technische Bundesanstalt  
 Attn: Peter Brenneke  
 Postfach 33 45  
 D-3300 Braunschweig  
 FEDERAL REPUBLIC OF GERMANY

D. R. Knowles  
 British Nuclear Fuels, plc  
 Risley, Warrington, Cheshire WA3 **6AS**  
 1002607 GREAT BRITAIN

Hahn-Meitner-Institut fur Kernforschung  
 Attn: Werner **Lutze**  
**Glienicker** Strasse 100  
 100 Berlin 39  
 FEDERAL REPUBLIC OF GERMANY

Institut fur **Tieflagerung** (4)  
 Attn: K. Kuhn  
 Theodor-Heuss-Strasse 4  
 D-3300 Braunschweig  
 FEDERAL REPUBLIC OF GERMANY

**Shingo Tashiro**  
 Japan Atomic Energy Research Institute  
**Tokai-Mura**, Ibaraki-Ken  
 319-11 JAPAN

Netherlands Energy Research Foundation  
**ECN (2)**  
 Attn: Tuen Deboer, Mgr.  
 L. H. Vons  
 3 Westerduinweg  
 P.O. Box 1  
 1755 **ZG Petten**, THE NETHERLANDS

Svensk Karnbransleforsorjning AB  
 Attn: Fred Karlsson  
 Project KBS  
 Karnbranslesakerhet  
 Box 5864  
 10248 Stockholm, SWEDEN

SANDIA INTERNAL

400 L. D. Tyler  
 1510 J. C. **Cummings**  
 1514 H. S. Morgan  
 1514 J. G. **Arguello**  
 3141 S. A. Landenberger (5)  
 3141 C. L. Ward, (8) for **DOE/OSTI**  
 3151 Supervisor (3)  
 6000 V. L. Dugan, Acting  
 6232 **W. R. Wawersik**  
 6233 J. C. Eichelberger  
 6233 J. L. **Krumhansl**  
 6257 J. **K. Linn**  
 6257 B. L. Ehgartner (10)  
 6300 T. O. Hunter, Acting  
 6310 T. E. Blejwas, Acting  
 6313 L. E. Shephard  
 6340 W. D. **Weart**  
 6340 S. Y. Pickering  
 63408 A. R. **Lappin**  
 6341 R. C. Lincoln  
 6341 Staff (9)  
 6341 **Sandia** WIPP Central Files (10)

6342 D. R. Anderson  
 6342 **Staff (11)**  
 6343 T. M. Schultheis  
 6343 Staff (2)  
 6344 **E. Gorham**  
 6344 **Staff (10)**  
 6345 B. M. Butcher, Acting  
 6345 **Staff (9)**  
 6346 J. R. Tillerson  
 6346 Staff (7)  
 8524 J. A. Wackerly (SNLL Library)  
 9300 J. E. Powell  
 9310 J. D. Plimpton  
 9320 M. J. **Navratil**  
 9325 L. J. **Keck**  
 9330 J. O. Kennedy  
 9333 O. Burchett  
 9333 J. W. **Mercer**  
 9334 P. D. Seward